UNIVERSIDADE FEDERAL DO CEARÁ
CENTRO DE CIÊNCIAS
DEPARTAMENTO DE BIOQUÍMICA E BIOLOGIA MOLECULAR
PROGRAMA DE PÓS-GRADUAÇÃO EM BIOQUÍMICA

THAIS FERREIRA NASCIMENTO

DEFENSINA NSD7 DE *Nicotiana suaveolens* ACOPLADA AO ÁCIDO FOSFATÍDICO: AVALIAÇÕES SOBRE O MECANISMO MOLECULAR ATRAVÉS DA ANÁLISE DE BIOQUÍMICA QUÂNTICA E SIMULAÇÕES DE DINÂMICA MOLECULAR.

FORTALEZA
2018

THAIS FERREIRA NASCIMENTO

DEFENSINA NSD7 DE *Nicotiana suaveolens* ACOPLADA AO ÁCIDO FOSFATÍDICO: AVALIAÇÕES SOBRE O MECANISMO MOLECULAR ATRAVÉS DA ANÁLISE DE BIOQUÍMICA QUÂNTICA E SIMULAÇÕES DE DINÂMICA MOLECULAR.

Dissertação de mestrado apresentado à coordenação de do Programa de Pós-Graduação em Bioquímica como requisito obrigatório para a obtenção do título de Mestre em Bioquímica pela Universidade Federal do Ceará.
Orientador: Prof. Dr. Bruno Anderson Matias da Rocha.
Coorientador: Prof. Dr. Valder Nogueira Freire.

FORTALEZA
2018

Dados Internacionais de Catalogação na Publicação
Universidade Federal do Ceará
Biblioteca Universitária
Gerada automaticamente pelo módulo Catalog, mediante os dados fornecidos pelo(a) autor(a)

N199d Nascimento, Thais Ferreira.
Defensina Nsd7 de Nicotiana suaveolens acoplada ao ácido fosfatídico: : avaliações sobre o mecanismo molecular através da análise de bioquímica quântica e simulações de dinâmica molecular. / Thais Ferreira Nascimento. – 2018.
58 f. : il. color.

Dissertação (mestrado) – Universidade Federal do Ceará, Centro de Ciências, Programa de Pós-Graduação em Bioquímica, Fortaleza, 2018.
Orientação: Prof. Dr. Bruno Anderson Matias da Rocha.
Coorientação: Prof. Dr. Valder Nogueira Freire.

1. Bioquímica Quântica. 2. Defensinas. 3. Dinâmica Molecular. I. Título.

CDD 572

THAIS FERREIRA NASCIMENTO

DEFENSINA NSD7 DE *Nicotiana suaveolens* ACOPLADA AO ÁCIDO FOSFATÍDICO: AVALIAÇÕES SOBRE O MECANISMO MOLECULAR ATRAVÉS DA ANÁLISE DE BIOQUÍMICA QUÂNTICA E SIMULAÇÕES DE DINÂMICA MOLECULAR.

Dissertação de mestrado apresentado à coordenação de do Programa de Pós-Graduação em Bioquímica como requisito obrigatório para a obtenção do título de Mestre em Bioquímica pela Universidade Federal do Ceará. Área de concentração: Bioquímica Vegetal.

Aprovada em: ___/___/_____.

BANCA EXAMINADORA

_____

Prof. Dr. Bruno Anderson Matias da Rocha (Orientador)

Universidade Federal do Ceará (UFC)

_____

Prof. Dr. Valder Nogueira Freire

Universidade Federal do Ceará (UFC)

_____

Prof. Dr. Ito Libertaro Barroso Neto

Centro Universitário Christus (UNICHRISTUS)

A Deus.

Aos meus pais, Lucidalva Ferreira Furtado e Antônio Pereira do Nascimento

AGRADECIMENTOS

O presente trabalho foi realizado com apoio da Coordenação de Aperfeiçoamento de Pessoal de Nível Superior - Brasil (CAPES) - Código de Financiamento 001.

À CAPES, pelo apoio financeiro com a manutenção da bolsa de auxílio.

Ao Prof. Dr. Bruno Anderson Matias da Rocha e ao Prof. Dr. Valder Nogueira Freire, pela excelente orientação.

Ao professor participante da banca examinadora Ito Liberato Barroso Neto pelo tempo, pelas valiosas colaborações, pelas sugestões e pela atenção que sempre apresentou em relação aos meus trabalhos desde a graduação até o presente momento.

Aos colegas da turma de mestrado e aos alunos de iniciação científica do Laboratório de Biofísica Aplicada, pelas reflexões, críticas e sugestões recebidas.

À toda minha família, principalmente à minha mãe, pelo incentivo a minha caminhada acadêmica e por sempre me apoiar em todos meus desafios ao longo dos anos.

Á todos meus amigos, pela companhia concedida nos momentos fáceis e difíceis nesses anos de mestrado.

“E o céu será tua casa, voará com tuas asas.

Não se abalará por pouco, amaremos feito loucos.

Será livre como nunca e sorrirá como sempre.

Reinaremos por direito e que assim seja feito.”

Dela Cruz.

RESUMO

As defensinas vegetais são peptídeos catiônicos compostos de 45-54 aminoácidos que desempenham um papel no sistema imunológico inato. As defensinas podem desempenhar vários papéis no organismo da planta, incluindo atividade antibacteriana, proteinase inibitória, e etc. As interações com membranas fosfolipídicas celulares são um componente chave do mecanismo da ação do peptídeo antimicrobiano. No presente trabalho calculamos as energias de interação resíduo-droga-resíduo da defensina de *Nicotiana sauveolens*, NsD7 usando métodos quânticos e simulação de dinâmica molecular para revelar dados estruturais e mecanismos moleculares não expostos na literatura. Os dados de entrada para os cálculos realizados neste estudo foram adquiridos a partir a estrutura de cristal de raios-X da defensina NsD7 de plantas complexada com ácido fosfatídico (PA) (PDB ID: 5KK4). Neste estudo, a energia de interação entre um par específico de resíduos de aminoácidos e o ligante foi obtida a partir de cálculos quânticos. Além disso, realizamos um estudo da simulação de MD para analisar a interação e a estabilidade das moléculas de NsD7 na presença e na ausência da molécula de ácido fosfatídico. A estratégia utilizada encontrou alguns resíduos adicionais que mostram significância na interação de monômeros de NsD7, além daqueles mencionados anteriormente na literatura, como Lys1, Arg5, Glu6, Arg40, Lys45 e Cys47. Por outro lado, os resultados corroboram com o estudo anterior, mostrando que Lys36: PA e Arg39: PA possuem alta interferência na energia de ligação do sistema. Além disso, notamos em nosso estudo que o resíduo Lys4 possui baixa energia repulsiva. No estudo anterior, o Lys4 não mostrou interferência na formação de oligômeros. A simulação de dinâmica molecular corroborou com dados experimentais, mostrando que, na ausência da molécula de PA, o sistema é incapaz de manter a estabilidade do sistema. Por outro lado, quando a molécula de PA está presente no sistema, o complexo NsD7: PA se torna estável. Os cálculos quânticos utilizados no trabalho atrelado as simulações de MD são capazes de descrever o perfil energético do sistema, assim como analisar a estabilidade do sistema como um todo.

Palavras-chave: Bioquímica Quântica. Defensina. Dinâmica Molecular.

ABSTRACT

Plant defensins are cationic peptide composed of 45-54 amino acids that play a role in innate immune system. The defensins may play several roles in the plant organism including antibacterial activity, proteinase inhibitory, etc. Interactions with cellular phospholipid membranes are a key component of the antimicrobial peptide mechanism. We calculated the residue-residue−drug interaction energies of NsD7 defensin using quantum methods and molecular dynamics simulation to reveal structural data and molecular mechanisms not exposed in the literature. The input data for the calculations performed in this study was the X-ray crystal structure of plant defensin NsD7 complexed with phospatidic acid (PA) (PDB ID: 5KK4). In this study, the interaction energy between a specific pair of amino acid residues and the ligand was achieved from quantum calculations. Also, we performed a molecular dynamic study to analyze the interaction and the stability of the NsD7 molecules in the presence or absence of the phosphatidic acid. The current strategy has found a few extra residues that show significance on the interaction of NsD7 monomers, beyond those previously mentioned in the literature, such as Lys1, Arg5, Glu6, Arg40, Lys45 and Cys47. On the other hand, the results corroborate with the previously, showing that Lys36:PA and Arg39:PA have high interference in the binding energy of the system. Also, we noticed in our study that the residue Lys4 have low repulsive energy. In the previously study, the Lys4 did not showed interference in the oligomer formation. The molecular dynamics simulation corroborated with experimental data, showing that in the absence of PA, the system is incapable to maintain the system stability. On the other hand, when PA molecule is present in the system, the complex NsD7:PA become stable. The quantum calculations used in this work coupled to MD simulations are capable of describing the energy profile of the system as well as the stability analysis of the system as a whole.

Keywords: Defensin. Molecular Dynamics. Quantum Biochemistry

LISTA DE FIGURAS

LISTA DE TABELAS

LISTA DE ABREVIATURAS E SIGLAS

BIRD	Binding site, Interaction energy, and Residues Domain
DFT	Density Functional Theory
GluCer	Glicosilceramida esfingolipídica
MD	Molecular Dynamics
MFCC	Molecular fractionation with conjugate caps
OPG	Osteoprotegerin
PA	Phosphatidic Acid
PDB	Protein Data Bank
PIP2/ (PI (4,5) P2)	Phosphatidylinositol 4,5-bisphosphate/ Fosfatidilinositol 4,5 Bisfosfato
QM	Quantum Mechanics
RANKL	Receptor Activator of Nuclear Factor kB Ligand
RMSD	Root-Mean-Square Deviation
TDDFT	Time Dependent Density Functional Theory
UFC	Universidade Federal do Ceará

SUMÁRIO

1 CAPÍTULO I: FUNDAMENTAÇÃO TEÓRICA

1.1 Peptídeos antimicrobianos

Os organismos vivos desenvolveram algumas estratégias para manter uma defesa eficiente contra patógenos. Um exemplo disso são os peptídeos antimicrobianos (AMPs, do inglês *antimicrobial peptides*), também conhecido como peptideos de defesa que são oligopeptídeos com um número variável (de cinco a mais de cem) de aminoácidos. A maioria dos AMPs tem a capacidade de matar patógenos microbianos diretamente, enquanto outros agem indiretamente modulando os sistemas de defesa do hospedeiro. Assim, os AMPs agem sob um amplo espectro de organismos assim como os vírus, fungos, bactérias, e etc. (BAHAR; REN, 2013). A descoberta dos AMPs ocorreu quando Dubos (1939) extraiu um agente antimicrobiano de uma cepa de *Bacillus* do solo. Este extrato foi eficiente em proteger os ratos da infecção por pneumococos (DUBOS; CATTANEO, 1939).

Historicamente, os AMPs também podem ser determinados como peptídeos catiônicos de defesa do hospedeiro [1] (BROWN; HANCOCK, 2006), peptídeos antimicrobianos aniônicos [2] (HARRIS; DENNISON; PHOENIX, 2009), peptídeos anfipáticos catiônicos [3] (GROENINK *et al*., 1999), AMPs catiônicos [4] (BRADSHAW, 2003), peptídeos de defesa do hospedeiro [5] (RIEDL; ZWEYTICK; LOHNER, 2011) e peptídeos antimicrobianos α-helicoidais [6] (HUANG; HUANG; CHEN, 2010). Uma das maiores e mais estudadas famílias de AMPs é a das defensinas com mais de centenas defensinas identificadas na literatura. As defensinas são potentes contra micróbios específicos, mas também algumas defensinas mostram um aumento sinérgico no intervalo antimicrobiano em combinação (MYGIND *et al*., 2005).

1.2 Aspectos estruturais e atividades antimicrobiana

Defensinas foram identificadas em muitos organismos, de insetos a humanos, incluindo plantas. Nas espécies vegetais, a defensina é codificada por famílias multigênicas e expressa em estresses bióticos e abióticos. Defensina é produzida em todas as partes das plantas, incluindo sementes, vagens, frutas, partes de flores, folhas, tubérculos, raízes e caules (TAM *et al*., 2015).

As defensinas vegetais são peptídeos catiônicos compostos de 45-54 aminoácidos, básicas, ricas em cisteína, encontradas em todo o reino vegetal e que desempenham um papel

no sistema imunológico inato (THOMMA; CAMMUE; THEVISSEN, 2002). Os membros da família defensin da planta compartilham um considerável nível de conservação em relação aos resíduos de aminoácido. Uma marca registrada é a conservação de uma seqüência de oito resíduos de cisteína os quais formam quatro pontes dissulfeto. Adicionalmente, dois resíduos de glicina nas posições 13 e 34, um resíduo aromático na posição 11 e um resíduo de ácido glutâmico na posição 29 são tipicamente conservados nas defensinas de plantas (LAY *et al*., 2003). É proposto que estas ligações dissulfeto conservadas servem para definir as propriedades físico-químicas das defensinas, como uma resistência extrema a altas temperaturas e ambientes ácidos (OEEMIG *et al*., 2012).

Além disso, algumas características estruturais importantes podem ser identificadas comparandoas defensinas: a maioria compartilha o mesmo motivo α / β estabilizado por cisteínas, composto de três cadeias β antiparalelas e uma α-hélice. Sua carga positiva em pH fisiológico parece estar relacionada à interação inicial com grupos de cabeça aniônica dos lipídios da membrana microbiana. As propriedades hidrofóbicas permitem a interação com o núcleo da membrana que permite a acomodação da proteína e conseqüentemente a ruptura da membrana.

Embora as defensinas tenham uma estrutura tridimensional razoavelmente conservada, a identidade da sequência de aminoácidos entre as diferentes defensinas vegetais é inferior a 35%. Acredita-se que esta ampla variedade na sequência de aminoácidos das defensinas proporcionou a grande diversidade em relação às atividades biológicas que as defensinas desempenham (VAN DER WEERDEN; ANDERSON, 2013).

As defensinas podem desempenhar vários papéis no organismo da planta incluindo atividade antibacteriana (CHEN *et al*., 2005; SEGURA *et al*., 1998; ZHANG; LEWIS, 1997), tolerância ao zinco (MIROUZE *et al*., 2006), atividade inibidora da proteinase (WIJAYA *et al*., 2000), atividade inibidora da α-amilase (BLOCH; RICHARDSON, 1991) e atividade bloqueadora do canal iônico (KUSHMERICK *et al*., 1998; SPELBRINK, 2004). Além das atividades anti-patogênicas, aos quais as defensinas exercem, essas são geralmente consideradas não-tóxicas para as células de plantas e mamíferos e, portanto, as defensinas de plantas e os peptídeos semelhantes à defensina têm atraído muita atenção como candidatos promissores para aplicações médicas e biotecnológicas (DE OLIVEIRA CARVALHO; MOREIRA GOMES, 2011).

1.3 Síntese e mecanismos de ação

A maioria das defensinas vegetais são sintetizadas como proteínas precursoras ou pelo processamento pós-traducional, o qual cliva o C-terminal maduro do péptido da defensina a partir do peptídeo sinal de secreção. Depois da síntese realizada no espaço intracelular, a maioria das defensinas é secretada para o espaço extracelular. Entetanto, algumas defensinas, como as defensinas florais, são direcionadas para o vacúolo. Depois desse processo inicia-se seu modo de ação sob o patógeno (ALMEIDA *et al*., 2002).

Apesar das defensinas realizarem as mesmas atividades, o modo de ação no organismo pode variar entre as defensinas. Alguns mecanismos de ação usados pelos peptídeos de defesa inatos são: peptídeos baseados nos modelos de carpete, bastão-barril ou poro toroidal (BROGDEN, 2005). Quando se trata de defensinas, os mecanismo intracelular de ação das defensinas ainda é incerto, e sugere-se que alguns deles podem interagir com alvos e processos intracelulares, devido à sua localização citoplasmática. Entretanto, foi estabelicidade em estudo anterior que alguns tipos de defensina vegetais se ligam às membranas plasmáticas de patógenos sensíveis com alta afinidade. Assim, as defensinas têm como alvo propriedades únicas de membranas do patógenos, gerando uma alta seletividade da sua ação (THEVISSEN *et al*., 2000).

1.4 Classificação

A classificação original das defensinas foi proposta por Broekaert *et al*. (1995) e foi baseada na habilidade ou inabilidade da defensina de inibir o crescimento de fungos, bem como o efeito que teve na morfologia dos fungos durante a inibição do crescimento. Isto foi baseado em 12 seqüências de defensina, quatro das quais se diferenciam por volta de sete aminoácidos (BROEKAERT *et al*., 1995). Basear a classificação puramente em características antifúngicas não foi eficiente, pois, como já citado anteriormente, as defensinas permeiam muitas outras atividades antimicrobianas. Essas defensinas foram simplesmente colocadas no grupo "não-antifúngico". Uma classificação adicional baseada na identidade percentual da sequência foi posteriormente proposta por Harrison *et al*. (1997) para explicar as defensinas recentemente identificadas. No entanto, isso foi baseado em dezessete seqüências e, portanto, não é apropriado para a classificação do grande número de sequências disponíveis até o

momento (HARRISON *et al*., 1997).

1.5 Interação defensina-ligante para a oligomerização

Estudos diferentes mostraram que a permeabilização ou ruptura da membrana é apenas um entre vários mecanismos envolvidos no combate ao patógeno, mas ainda assim a membrana microbiana é a primeira barreira que deve ser superada (JANISIEWICZ *et al*., 2008; MARCOS *et al*., 2008). Além disso, adicionando outro quebra-cabeça às relações estrutura-dinâmica-função da família defensinas, foi proposto em diferentes trabalhos que a oligomerização é um requisito necessário para a permeabilização da membrana. Assim, pode-se observar que a dimerização e a oligomerização foi detectada em diversas defensinas de plantas. (DE BEER; VIVIER, 2011; POON *et al*., 2014).

Recentes estudos provaram que alguns esfingolipídeos mostraram ser alvos para várias várias defensinas de plantas (DE MEDEIROS *et al*., 2014; POON *et al*., 2014; SAGARAM *et al*., 2013). Esses trabalhos sugerem que existem várias vias para permitir o reconhecimento e o seqüestro de esfingolipídeos pelas defensinas na imunidade inata das plantas, assim apoiando a ideia de que diferentes esfingolipídeos podem agir nas células-alvo como sinalizadores de reconhecimento para desencadear o mecanismos de imunidade inatos da plantas a partir da ação das defensina (KVANSAKUL *et al*., 2016).

No estudo com a defensina NaD1 foi demonstrado que a dimerização da defensina NaD1 aumentou sua atividade antifúngica. Esse efeito foi atribuído à presença de uma área de superfície com carga positiva prolongada no dímero da NaD1 que pode ser importante para a ligação inicial às glicoproteínas carregadas negativamente que estão localizadas nas paredes das células fúngicas (LAY *et al*., 2012). Nesse caso, os ensaios de bandas lipídicas revelaram que o NaD1 é capaz de interagir com um lipídio da membrana, o fosfatidilinositol 4,5 bisfosfato (PI (4,5) P2), e também, no mesmo estudo foi resolvido a estrutura cristalina do complexo NaD1- (PI (4,5) P2.

Eles descreveram um único oligômero em forma de arco composto de sete dímeros de NaD1 que unem-se cooperativamente com os grupos de cabeças aniônicas de 14 moléculas PI (4,5) P2 através de uma configuração única de "aderência catiônica". Essas observações levaram à hipótese de que o NaD1 permeabiliza as células formando um complexo com PI (4,5) P2 no folheto interno da membrana plasmática que leva a ruptura de membrana,

possivelmente pela ruptura das interações citoesqueleto-membrana que ocorrem através do PI (4,5) P2 (POON *et al*., 2014).

Também é possível citar outras interações entre defensinas-ligantes para a formação do oligômero e posterior ação contra patógenos. No primeiro exemplo, foi demonstrado a interação entre a defensina de ervilha PsD1 e membranas contendo o glicosilceramida esfingolipídica (GluCer).

Estas análises revelaram uma maior afinidade de PsD1 pelas membranas contendo GluCer, com rápida cinética de associação e dissociação e uma alteração na conformação da defensina associada à ligação de GluCer (DE MEDEIROS *et al*., 2014). No segundo caso, foi observado que defensina MtDef4 do Medicago truncatula interage com o ácido fosfatídico (PA). Entretando, a defensina MtDef4 não interage somente com o ligante PA, mas também se liga aos fosfatos do fosfatidilinositol, especialmente o PI (3,5) P2 (SAGARAM *et al*., 2013).

1.6 Complexo NsD7-ácido fosfatídico

Estudo recente revelou a estrutura cristalina da defensina NsD7, um homólogo de NaD1 clonado de *N. suaveolens* (91,5% idêntico ao NaD1), complexada ao ácido fosfatídico (PA, do inglês *Phosphatidic Acid*) (NsD7-PA; pdb: 5KK4). Este estudo revelou que o complexo é composto por uma dupla hélice de duas fibrilas de defensina oligoméricas enroladas para a direita, demonstrando que este complexo adota uma topologia radicalmente diferente, comparada com o complexo NaD1: PIP2 (PAYNE *et al*., 2016). Kvansakul *et al* (2016) realizaram mutagênese dirigida no complexo utilizando três alvos: (i) o sítio de ligação ao PA do tipo I, que a molécula de PA interage na junção entre dois dímeros NsD7 vizinhos; (ii) sítio de ligação ao PA do tipo II, em que o PA interage numa aderência catiônica formada por cada dímero de NsD7, (iii) fecho de isoleucina, localizado no interior da hélice dupla do oligômero e (iv) região interoligomérica.

Suas descobertas revelaram que a montagem do complexo depende da interação com PA na interface entre os dímeros de NsD7. Além disso, eles indicaram que os resíduos de defensina que definem a estabilidade do complexo NsD7: PA diferem para o acoplamento lipídico e para os contatos dímero: dímero (KVANSAKUL *et al*., 2016).

Considerando o estudo de Kvansakul *et al* (2016) sobre a oligomerização do complexo

NsD7-PA e a permeabilização da membrana, foi proposto que os mecanismos de ação previamente sugeridos para AMPs (modelos de carpete, bastão barril ou poro toroidal) (BROGDEN, 2005) são inaplicável ao sistema NsD7. Os novos dados sugerem um modelo de ruptura de membrana através de um mecanismo de desestabilização direta envolvendo o sequestro de PA por interação após a oligomerização de NsD7 (KVANSAKUL *et al*., 2016).

2 MÉTODOS COMPUTACIONAIS

Os avanços na computação e tecnologias relacionadas permitem simular sistemas físicos em escala atomística inatacáveis poucas décadas atrás. A modelagem computacional, ou experimentação *in silico*, desempenha, atualmente, papel fundamental na investigação e compreensão das propriedades de sistemas nanométricos e na construção de novas moléculas com potencial farmacológico e na compreensão das interações moleculares que ocorrem em sistemas biológicos. A evolução do poder computacional, tanto do ponto de vista de hardware quanto do desenvolvimento de algoritmos, e níveis teóricos cada vez mais detalhados baseados na estrutura eletrônica, tornou factível a simulação das propriedades físicas e químicas dos fármacos. O processamento em paralelo e o incremento da capacidade dos métodos teóricos e do software têm levado a resultados marcantes nos cálculos de propriedades estruturais, eletrônicas, ópticas e dinâmicas (mais recentemente) de sistemas complexos biológicos (SHERRILL, 2010)

Métodos quânticos de primeiros princípios e dinâmica molecular são ferramentas úteis para a investigação de receptores biológicos e ligantes bioativos (COLE *et al*., 2010; DE BENEDETTI; FANELLI, 2010; SÖDERHJELM *et al*., 2010). A Teoria do Funcional da Densidade (DFT, do inglês *Density Functional Theory*) tem obtido enorme sucesso no estudo das interações entre ligantes e proteínas com base em um ponto de vista atomístico-eletrônico (SAHAI; BIGGIN, 2011; SALAZAR; SEMINARIO, 2008; SUN; SCOTT, 2010)

Ela fornece informações sobre os rearranjos eletrônicos consequentes das ligações bioativas realizadas, a estrutura e a energia relativa do ligante ao sítio de ligação, entre outras propriedades. A Teoria do Funcional da Densidade Dependente do Tempo (TDDFT, do inglês *Time Dependent Density Functional Theory*) (PETERSILKA; GOSSMANN; GROSS, 1996) permite o estudo de processos relacionados a estados excitados como reações fotoeletroquímicas e luminescência.

A Dinâmica Molecular (MD, do inglês *Molecular Dynamics*), que se refere ao uso de funções energia potencial simples (e.g., oscilador harmônico ou potenciais Coulombianos) para a modelagem de sistemas moleculares, pode ser aplicada na investigação de uma larga gama de fenômenos de larga escala, incluindo aqueles de bioquímica estrutural, biofísica, enzimologia, biologia molecular, química farmacêutica e biotecnologia (KLEIN; SHINODA, 2008). Em particular, a Dinâmica Molecular fornece a possibilidade da realização de design molecular de drogas e proteínas, e determinação e refino de estruturas moleculares (raios X, NMR e modelagem).

A Dinâmica Molecular foi incluída análise das propriedades dinâmicas entre proteína-proteína e proteína-ligante. A importância da dinâmica de proteínas no processo de interação ganhou grande atenção nos últimos anos. A possibilidade de medir movimentos na escala temporal de nanosegundos (ns) a microssegundos (ms) é capaz de revelar a complexidade do conjunto de conformação de proteínas em solução (BRÜSCHWEILER, 2003; HENZLER-WILDMAN; KERN, 2007; PALMER III, 2001). Estudos recentes sobre a dinâmica de proteínas levaram à percepção de que as proteínas não são estruturadas em uma única conformação; em vez disso, elas frequentemente exibem regiões onde há mudanças conformacionais. A visão inovadora sob ligação e interação entre aminoácidos leva em consideração o equilíbrio entre estados conformacionais pré-existentes da proteína antes de encontrar o ligante. Na forma complexada (proteína-ligante) nenhuma transição conformacional significativa é necessária; em vez disso, há um deslocamento dos átomos em direção ao estado conformacional referente à proteína-ligante. Várias evidências mostraram que regiões que exibem mudança conformacional participam diretamente das interações ou das transições alostéricas (JAMES; TAWFIK, 2003; VOLKMAN *et al*., 2001).

2.1 Dinâmica Molecular aplicada às defensinas

Quase todos os processos biológicos realizados pelas proteínas dependem de sua flexibilidade. Simulações de dinâmica molecular fornecem pontos de vista apropriados para a modelagem da estrutura microscópica na escala atômica e molecular. As forças e energias de um sistema molecular podem ser avaliadas em simulações computacionais. A simulação de dinâmica molecular é uma técnica para investigar a relação entre a estrutura molecular e os movimentos moleculares, por isso este método pode ser utilizado para compreender a função das macromoléculas biológicas. Embora a simulação de dinâmica molecular não possa ser

suplantada com os métodos experimentais, ela pode ser um bom complemento para os métodos experimentais, afim de revelar dados ainda não apresentados na literatura (ADCOCK; MCCAMMON, 2006). Aqui apresentamos alguns estudos reportados na literatura que revelam o quão produtiva pode ser a dinâmica molecular aplicada às defensinas.

No primeiro caso, uma nova defensina proveniente de uma proteína recombinante (SDmod) de sistema eucariótico foi produzida e, assim foi comparada a absorção dos íons cádmio pela forma oxidada e reduzida desta nova defensina a partir de avaliação experimental e simulação MD. A proteína recombinante SDmod é proveniente de um gene de defensina vegetal modificado utilizado para alcançar uma gama mais ampla de atividades da defensina, com base na sequência do gene SD2 da defensina do girassol.(SOTCHENKOV *et al*., 2005).

No segundo caso, um estudo mostrou que o PW2, um peptídeo anticocidial, em solução não é completamente flexível. As distâncias medidas no estudo revelaram o movimento restrito na região aromática (Trp-Trp-Arg) e a simulação dinâmica molecular de 10ns em água mostraram o aumento dos parâmetros de ordem nessa mesma região (CRUZEIRO-SILVA *et al*., 2007).

No último caso, o trabalho realizado permitiu determinar a estrutura em alta resolução, indicando a presença da cadeia principal e da cadeia lateral notavelmente bem definidas para a maioria dos resíduos em PsDef1. A estrutura demonstra que, similarmente a outras defensinas vegetais, PsDef1 adota a dobra CSαβ que consiste de três cadeias beta formando uma folha beta anti-paralela, e uma hélice α que se dobra no topo da folha-beta (DE MEDEIROS *et al*., 2010, 2014).

2.2 Mecânica Quântica aplica à interação proteína-proteína

Simulações computacionais em nível quântico vêm sendo empregadas nos últimos anos para entender os diversos mecanismos de ligação e as propriedades físico- químicas de sistemas biológicos.

Souza *et al.* aplicou com sucesso o método QM para o cálculo de interações individuais resíduo-resíduo em sistemas biológicos. O trabalho citado revelou uma descrição energética detalhada de todos os resíduos provenientes da interação proteína-proteína envolvidos no estabelecimento do complexo RANKL (do *inglês Receptor Activator of Nuclear Factor kB Ligand*) -OPG (do inglês *Osteoprotegerin*) aprofundando o conhecimento

sobre a inibição da osteoclastogênese e destacando o núcleo tripeptídico, como a chave para a funcionalidade da OPG (SOUSA *et al*., 2016).

Neste trabalho, estabelecemos pela primeira vez uma nova estratégia que designa a interação energética do sistema resíduo-ligante-resíduo utilizando o método de mecânica quântica aplicado à sistemas protéicos. Através desse método é possível revelar o perfil energético do sistema em questão, pois o cálculo realizado inclui as energias individuais de cada aminoácido atrelado a energia do ligante que está presente no sistema.

Em relação as defensinas, a literatura já mostrou estudos nesses sistemas envolvendo simulações em MD (DE MEDEIROS *et al*., 2010; SOTCHENKOV *et al*., 2005). Entretanto, até o presente momento não foram apresentados dados de estudos quânticos aplicados a defensinas.

3 CONCLUSÃO

A análise atual delineia uma descrição energética detalhada do complexo NsD7-PA, aprofundando o conhecimento sobre o sistema imune da defensina, NsD7. Além disso, nossos resultados forneceram uma base estrutural e energética da defensina NsD7. Desta forma, é possível estender a mesma abordagem a outras defensinas, a fim de ampliar o conhecimento sobre o sistema imune das plantas com a intenção de melhorar-ló.

Cálculos quânticos confirmaram a importância da molécula de PA na oligomerização principalmente através dos resíduos que interagem com a molécula de PA no sistema. Isso foi observado através dos resíduos Lys36 e Arg39, pois estes apresentaram alta energia de interação. Essas suposições corroboram com o trabalho de Kvansakul *et al*. (2016), que realizaram uma pesquisa experimental utilizando mutagênese sítio-dirigida para provar que os resíduos Lys36 e Arg39 são importantes na formação oligômero-fibrila (KVANSAKUL *et al*., 2016). Além disso, outros resíduos, nunca mencionados na literatura, tiveram sua importância revelada na análise de QM, tais como: Lys1 (-29,6 kcal mol-1), Arg5 (-36,4 kcal mol-1), Glu6 (-19,0 kcal mol-1), Arg40 (-24,0 kcal mol-1), Lys45 (-22,0 kcal mol-1) e Cys47 (-26,0 kcal mol-1). Esses resíduos mostraram energia de ligação atrativa, o que sugere que eles promovem uma maior estabilidade dos dímeros de NsD7. Todos esses fatos enfatizam o papel crucial desses resíduos em conjunto com a molécula de PA na importância na montagem e estabilização do complexo NsD7-PA.

Após a realização da mecânica quântica, também realizamos simulação clássicas através da MD, mostrando que na ausência da molécula de PA houve rupturas nas interações entre resíduos, ocasionando o descolamento entre os dímeros. Quando comparado com a simulação do complexo NsD7-PA, o NsD7 por si só mostrou mudanças mais abruptas na sua conformação de estrutura secundária. Isso levou à instabilidade do sistema comprovada pelo gráfico RMSD, que pode causar um impacto severo na funcionalidade da defensina. No geral, nossos resultados demonstram, pela primeira vez, que o novo método QM aplicado ao sistema NsD7 é prático para elucidar dados moleculares nunca mostrados na literatura anterior.

Além disso, as técnicas computacionais no nível quântico, em conjunto com métodos clássicos de dinâmica molecular, podem ser muito úteis para fornecer dados moleculares que determinam a eficácia das defensinas e, assim, possibilitar o uso em muitos campos como biotecnologia, agricultura e aplicações médicas. No futuro, ambas as abordagens deverão buscar alternativas moléculas que possam interagir com defensinas e promovam a

oligomerização em outros sistemas de defensinas, expandindo o conhecimento das defensinas e, assim, melhorando o sistema imunológico das plantas.

REFERÊNCIAS

ADCOCK, S. A.; MCCAMMON, J. A. Molecular dynamics: Survey of methods for simulating the activity of proteins**. Chemical Reviews**, La Jolla, v. 106, n. 5, p 1589-1615 2006.

BAHAR, A. A.; REN, D. **Antimicrobial Peptides**. Syracuse, v. 6, n. 12, p. 1543-1575, 2013.

BLOCH, C.; RICHARDSON, M. A new family of small (5 kDa) protein inhibitors of insect alpha-amylases from seeds or sorghum (Sorghum bicolar (L) Moench) have sequence homologies with wheat gamma-purothionins. **FEBS letters**, Durham v. 279, n. 1, p. 101-104, 1991.

BOMAN, H. G.; HULTMARK, D. Cell-free immunity in insects. **Trends in Biochemical Sciences**, New York, v. 6, p. 306-309, 1981.

BRADSHAW, J. Cationic antimicrobial peptides : issues for potential clinical use. **BioDrugs : clinical immunotherapeutics, biopharmaceuticals and gene therapy**, Edinburgh v. 17, n. 4, p. 233-240, 2003.

BROEKAERT, W. F. *et al*. Plant defensins: novel antimicrobial peptides as components of the host defense system. **Plant physiology**, Heverlee, v. 108, n. 4, p. 1353-1358, 1995.

BROGDEN, K. A. Antimicrobial peptides: Pore formers or metabolic inhibitors in bacteria. **Nature Reviews Microbiology**, Iowa City, v. 3, p. 238-250, 2005.

BROWN, K. L.; HANCOCK, R. E. W. Cationic host defense (antimicrobial) peptides**. Current Opinion in Immunology**, British Columbia, v. 18, n. 1, p 24-30, 2006.

BRÜSCHWEILER, R. New approaches to the dynamic interpretation and prediction of NMR relaxation data from proteins. **Current Opinion in Structural Biology**, Worcester, v. 13, n. 2, p. 175-183, 2003.

CHEN, G. H. *et al*. Cloning and characterization of a plant defensin VaD1 from azuki bean. **Journal of Agricultural and Food Chemistry**, Taiwan, v. 53, n. 4, p. 982-988, 2005.

COLE, D. J. *et al*. Protein-protein interactions from linear-scaling first-principles quantum-mechanical calculations. **EPL**, Cambridge, v. 91, n. 3, 2010.

CRUZEIRO-SILVA, C. *et al*. Structural biology of membrane-acting peptides: Conformational plasticity of anticoccidial peptide PW2 probed by solution NMR. **Biochimica et Biophysica Acta - Biomembranes**, Rio de Janeiro, v. 1768, n. 12, p. 3182-3192, 2007.

DE BENEDETTI, P. G.; FANELLI, F. Computational quantum chemistry and adaptive ligand modeling in mechanistic QSAR. **Drug Discovery Today**, Módena, v. 15, n. 19-20, p. 859-866, 2010.

DE MEDEIROS, L. N. *et al*. Backbone dynamics of the antifungal Psd1 pea defensin and its correlation with membrane interaction by NMR spectroscopy. **Biochimica et Biophysica Acta - Biomembranes**, Rio de Janeiro, v. 1798, n. 2, p. 105-113, 2010.

DE MEDEIROS, L. N. *et al*. Psd1 binding affinity toward fungal membrane components as assessed by SPR: The role of glucosylceramide in fungal recognition and entry Biopolymers - **Peptide Science Section**, Rio de Janeiro, v. 102, n. 6, p. 456-464, 2014

DE OLIVEIRA CARVALHO, A.; MOREIRA GOMES, V. Plant Defensins and Defensin-Like Peptides - Biological Activities and Biotechnological Applications. **Current Pharmaceutical Design**, New York, v. 17, n. 38, p. 4270-4293, 2011.

DUBOS, R. J.; CATTANEO, C. Studies on a bactericidal agent extracted from a soil bacillus : iii. Preparation and activity of a protein-free fraction. **The Journal of experimental medicine**, Campos dos Goytacazes, v. 70, n. 3, p. 249-256, 1939.

ERMAKOVA, E. A. *et al*. Structure of Scots pine defensin 1 by spectroscopic methods and computational modeling. **International Journal of Biological Macromolecules**, Kazan, v. 84, p. 142-152, 2016.

GROENINK, J. *et al*. Cationic amphipathic peptides, derived from bovine and human lactoferrins, with antimicrobial activity against oral pathogens. **FEMS Microbiology Letters**, Amsterdam, v. 179, n. 2, p. 217-222, 1999.

HARRIS, F.; DENNISON, S.; PHOENIX, D. Anionic Antimicrobial Peptides from Eukaryotic Organisms. **Current Protein & Peptide Science**, Preston, v. 10, n. 6, p. 585-606, 2009.

HARRISON, S. J. *et al*. An antimicrobial peptide from the Australian native Hardenbergia violacea provides the first functionally characterised member of a subfamily of plant defensins. **Australian Journal of Plant Physiology**, *[s.l]* v. 24, n. 5, p. 571-578, 1997.

HENZLER-WILDMAN, K.; KERN, D. Dynamic personalities of proteins. **Nature**, Brandeis University, Waltham, v. 450, p. 964-972, 2007.

HÖGLUND, P.; LJUNGGREN, H. G. Natural killer cells in cancer. **Natural Killer Cells**. *[s.l: s.n.]*. p. 55-64.

HUANG, Y.; HUANG, J.; CHEN, Y. Alpha-helical cationic antimicrobial peptides: Relationships of structure and function**. Protein and Cell**, Changchun, v.1, n.2, p. 143-152, 2010.

JAMES, L. C.; TAWFIK, D. S. Conformational diversity and protein evolution - A 60-year - old hypothesis revisited. **Trends in Biochemical Sciences**, Cambridge, v. 28, n. 7, p.361-368, 2003.

JANISIEWICZ, W. J. *et al*. Improved biocontrol of fruit decay fungi with Pichia pastoris recombinant strains expressing Psd1 antifungal peptide. **Postharvest Biology and Technology**, Kearneysville, v. 47, n. 2, p. 218-225, 2008.

KLEIN, M. L.; SHINODA, W. Large-scale molecular dynamics simulations of self-assembling systems. **Science.** New York, v. 321, n. 5890, p. 798-800, 2008.

KUSHMERICK, C. *et al*. Functional and structural features of gamma-zeathionins, a new class of sodium channel blockers. **Febs Letters**, Belo Horizonte, v. 440, n. 3, p. 302-306, 1998.

KVANSAKUL, M. *et al*. Binding of phosphatidic acid by NsD7 mediates formation of helical defensin-lipid oligomeric assemblies and membrane permeabilization. **Proceedings of the National Academy of Sciences of the United States of America**, Melbourne, v. 113, n. 40, p. 11202-11207, 2016.

LAY, F. T. *et al*. The three-dimensional solution structure of NaD1, a new floral defensin from Nicotiana alata and its application to a homology model of the crop defense protein alfAFP. **Journal of Molecular Biology**, Victoria, v. 325, n. 1, p. 175-188, 2003.

LAY, F. T. *et al*. Dimerization of plant defensin NaD1 enhances its antifungal activity. **Journal of Biological Chemistry**, Melbourne v. 287, n. 24, p. 19961-19972, 2012.

MARCOS, J. F. *et al*. Identification and Rational Design of Novel Antimicrobial Peptides for Plant Protection. **Annual Review of Phytopathology**, Burjassot, v. 46, n. 1, p. 273-301, 2008.

MIROUZE, M. *et al*. A putative novel role for plant defensins: A defensin from the zinc hyper-accumulating plant, Arabidopsis halleri, confers zinc tolerance. **Plant Journal**, Auzeville-Tolosane, v. 47, n. 3, p. 329-342, 2006.

MYGIND, P. H. *et al*. Plectasin is a peptide antibiotic with therapeutic potential from a saprophytic fungus. **Nature**, Bagsvaerd, v. 437, n. 7061, p. 975-980, 2005.

OEEMIG, J. S. *et al*. Eurocin, a New Fungal Defensin. **Journal of Biological Chemistry**, Aalborg v. 287, n. 50, p. 42361-42372, 2012.

PALMER III, A. G. NMR Probes of Molecular Dynamics: Overview and Comparison with Other Techniques. **Annual Review of Biophysics and Biomolecular Structure**, *[s.l]*, v. 30, n. 1, p. 129-155, 2001.

PAYNE, J. A. E. *et al*. The plant defensin NaD1 introduces membrane disorder through a specific interaction with the lipid, phosphatidylinositol 4,5 bisphosphate. **Biochimica et Biophysica Acta - Biomembranes**, Melbourne, v. 1858, n. 6, p. 1099-1109, 2016.

PETERSILKA, M.; GOSSMANN, U.; GROSS, E. Excitation Energies from Time-Dependent Density-Functional Theory. **Physical Review Letters**, Berkeley, v. 76, n. 8, p. 1212-1215, 1996.

POON, I. K. H. *et al*. Phosphoinositide-mediated oligomerization of a defensin induces cell lysis. **eLife**, Melbourne, v. 2014, n. 3, 2014.

RIEDL, S.; ZWEYTICK, D.; LOHNER, K. Membrane-active host defense peptides: challenges and perspectives for the development of novel anticancer drugs. **Chemistry and physics of lipids**, Schmiedlstrasse, v. 164, n. 8, p. 766-781, 2011.

SAGARAM, U. S. *et al*. Structural and functional studies of a phosphatidic acid-binding

antifungal plant defensin MtDef4: Identification of an RGFRRR motif governing fungal cell entry. **PLoS ONE**, Saint Louis, v. 8, n. 12, 2013.

SAHAI, M. A.; BIGGIN, P. C. Quantifying water-mediated protein-ligand interactions in a glutamate receptor: A DFT study. **Journal of Physical Chemistry B**, Schmiedlstrasse, v. 115, n. 21, p. 7085-7096, 2011.

SALAZAR, P. F.; SEMINARIO, J. M. Identifying receptor-ligand interactions through an ab initio approach. **Journal of Physical Chemistry B**, College Station, v. 112, n. 4, p. 1290-1292, 2008.

SEGURA, A. *et al*. Novel defensin subfamily from spinach (Spinacia oleracea). **FEBS Letters**, Madrid, v. 435, n. 2-3, p. 159-162, 1998.

SHERRILL, C. D. Frontiers in electronic structure theory. **The Journal of Chemical Physics**, Atlanta, v. 132, n. 11, p. 110902, 2010.

SÖDERHJELM, P. *et al*. Estimates of ligand-binding affinities supported by quantum mechanical methods**. Interdisciplinary Sciences: Computational Life Sciences**, Lund, v. 2, n. 1, p. 21-37, 2010.

SOTCHENKOV, D. V. *et al*. Modification of the sunflower defensin SD2 gene sequence and its expression in bacterial and yeast cells. **Russian Journal of Genetics**, v. 41, n. 11, p. 1194-1201, 2005.

SOUSA, B. L. *et al*. Explaining RANKL inhibition by OPG through quantum biochemistry computations and insights into peptide-design for the treatment of osteoporosis. **Rsc Advances**, Moscow, v. 6, n. 88, p. 84926-84942, 2016.

SPELBRINK, R. G. Differential Antifungal and Calcium Channel-Blocking Activity among Structurally Related Plant Defensins. **Plant physiology**, St. Louis, v. 135, n. 4, p. 2055-2067, 2004.

SUN, H.; SCOTT, D. O. Structure-based drug metabolism predictions for drug design**. Chemical Biology and Drug Design**, Groton, v. 75, n. 1, p. 3-17, 2010.

TAM, J. P. *et al*. Antimicrobial peptides from plants. **Pharmaceuticals**, Singapore, v. 8, n. 4, p.711-757, 2015.

THEVISSEN, K. *et al*. Specific Binding Sites for an Antifungal Plant Defensin from Dahlia (*Dahlia merckii*) on Fungal Cells Are Required for Antifungal Activity. **Molecular Plant-Microbe Interactions**, Heverlee-Leuven, v. 13, n. 1, p. 54-61, 2000.

THOMMA, B. P. H. J.; CAMMUE, B. P. A.; THEVISSEN, K. Plant defensins. **Planta**, Heverlee-Leuven, v. 216, n. 2, p. 193-202, 2002.

VAN DER WEERDEN, N. L.; ANDERSON, M. A. Plant defensins: Common fold, multiple functions. **Fungal Biology Reviews**, Melbourne, v. 26, n. 4, p. 121-131, 2013.

VOLKMAN, B. F. *et al*. Two-state allosteric behavior in a single-domain signaling protein.

Science, Madison, v. 291, n. 5512, p. 2429-2433, 2001.

WANG, G. Improved methods for classification, prediction, and design of antimicrobial peptides. **Computational Peptidology**. *[s.l: s.n.*]. p. 43-66.

WIJAYA, R. *et al*. Defense proteins from seed of Cassia fistula include a lipid transfer protein homologue and a protease inhibitory plant defensin. **Plant Science**, Bundoora, v. 159, n. 2, p. 243-255, 2000.

ZHANG, Y.; LEWIS, K. Fabatins: New antimicrobial plant peptides. **FEMS Microbiology Letters**, *[s.l]* v. 149, n. 1, p. 59-64, 1997.

4 CAPÍTULO II: NSD7 DEFENSIN BINDING TO PHOSPATIDIC ACID: INSIGHTS ON MOLECULAR MECHANISM THROUGH QUANTUM BIOCHEMISTRY AND MOLECULAR DYNAMICS SIMULATIONS

Plant defensins are cationic peptide composed of 45-54 amino acids that play a role in innate immune system. The defensins may play several roles in the plant organism including antibacterial activity, proteinase inhibitory, etc. Interactions with cellular phospholipid membranes are a key component of the antimicrobial peptide mechanism. We calculated the residue-residue−drug interaction energies of NsD7 defensin using quantum methods and molecular dynamics simulation to reveal structural data and molecular mechanisms not exposed in the literature.

The input data for the calculations performed in this study was the X-ray crystal structure of plant defensin NsD7 complexed with phospatidic acid (PA) (PDB ID: 5KK4). In this study, the interaction energy between a specific pair of amino acid residues and the ligand was achieved from quantum calculations. Also, we performed a molecular dynamic study to analyze the interaction and the stability of the NsD7 molecules in the presence or absence of the phosphatidic acid. The current strategy has found a few extra residues that show significance on the interaction of NsD7 monomers, beyond those previously mentioned in the literature, such as Lys1, Arg5, Glu6, Arg40, Lys45 and Cys47.

On the other hand, the results corroborate with the previously, showing that Lys36:PA and Arg39:PA have high interference in the binding energy of the system. Also, we noticed in our study that the residue Lys4 have low repulsive energy. In the previously study, the Lys4 did not showed interference in the oligomer formation.

The molecular dynamics simulation corroborated with experimental data, showing that in the absence of PA, the system is incapable to maintain the system stability. On the other hand, when PA molecule is present in the system, the complex NsD7:PA become stable. The quantum calculations used in this work coupled to MD simulations are capable of describing the energy profile of the system as well as the stability analysis of the system as a whole.

5 INTRODUCTION

The living organisms have developed some strategies such as natural killer cells, antibodies and defensins to maintain an efficient defense against pathogens (BOMAN; HULTMARK, 1981; HÖGLUND; LJUNGGREN, 2010). Antimicrobial peptides have less than 100 amino acids and, based on structural informations, they are classified into four categories: (1) cysteine-rich amphiphilic β -sheet peptides; (2) amphiphilic a-helical peptides; (3) cysteine-disulfide ring peptides; and (4) linear peptides with one or two predominant amino acids (WANG, 2015). Defensins are cysteine-rich antimicrobial peptides with a triple-stranded β -sheet structure connected with a loop of β -hairpin turn. Plant defensins are cationic peptide composed of 45-54 amino acids that play a role in innate immune system (THOMMA; CAMMUE; THEVISSEN, 2002).

Defesins have an identical backbone structure stabilized by four or five intramolecular of plant defensins has shown that the structure comprises a triple-stranded β -sheet with an α -helix in parallel (Figure 2). Although defensins have a reasonably conserved three-dimensional structure (Figure 1), the amino acid sequence identity between different plant defensins is less than 35%.

Figure 1 - Sequence alignment of defensins NsD7-PA, NsD7-PIP2, NaD1, MtDef4, VrD2, Psd1, Rs-AFP1, Rs-AFP2, PsDef1 and Vrd1. Identical residues are colored yellow, representing cysteines residue which are conserved in primary structure of defensins. Positive and negative residues are colored blue and red, respectively. The lines represent disulfide bridges of conserved cysteines. At the top, the arrows represent triple-stranded *β* sheet and the

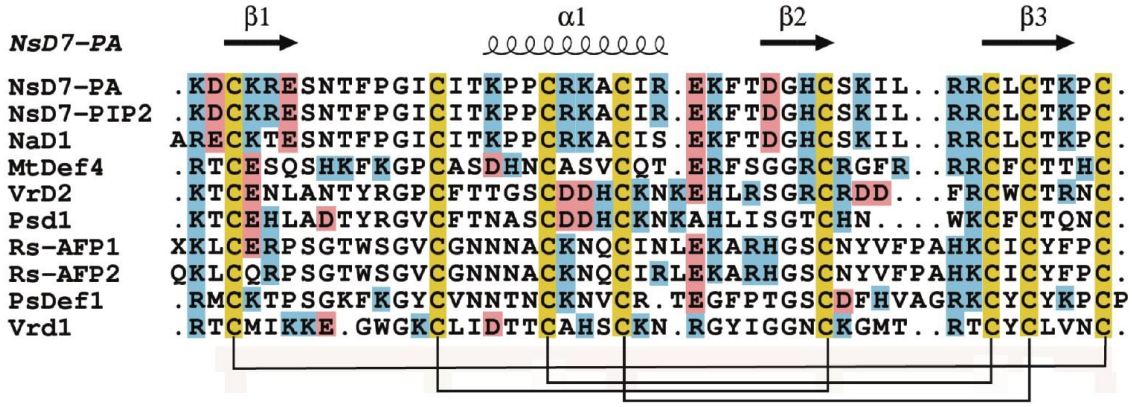

Source: Prepared by the author

rim represent α -helix in NsD7-PA complex.

It is believed that this wide variety in the amino acid sequence of the defensins provided the great diversity in relation to the biological activities that the defensins play (ERMAKOVA *et al*., 2016).

The defensins may play several roles in the plant organism including antibacterial activity (CHEN *et al*., 2005; SEGURA *et al*., 1998; ZHANG; LEWIS, 1997), zinc tolerance (MIROUZE *et al*., 2006), proteinase inhibitory activity (WIJAYA *et al*., 2000), α -amylase inhibitory activity (BLOCH; RICHARDSON, 1991) and ion channel blocking activity (KUSHMERICK *et al*., 1998; SPELBRINK, 2004). Despite defensins perform the same activities the mode of action on the organism may vary among defensins.

Some mechanisms of action used by innate defense peptides are: peptides based on the carpet, barrel-stave, or toroidal-pore models. When it comes to defensins, the mechanisms of

Figure 2 - Cartoon representation of defensins (a) NsD7-PA, (b) NsD7-PIP2, (c) NaD1, (d) MtDef4, (e) VrD2, (f)Psd1, (g) Rs-AFP1, (h) Rs-AFP2, (i) PsDef1 and (j) Vrd1. The quaternary structure of all defensins exposed comprises a triple-stranded β –sheet (colored in violet, orange and yellow) with an α –helix (colored in green).

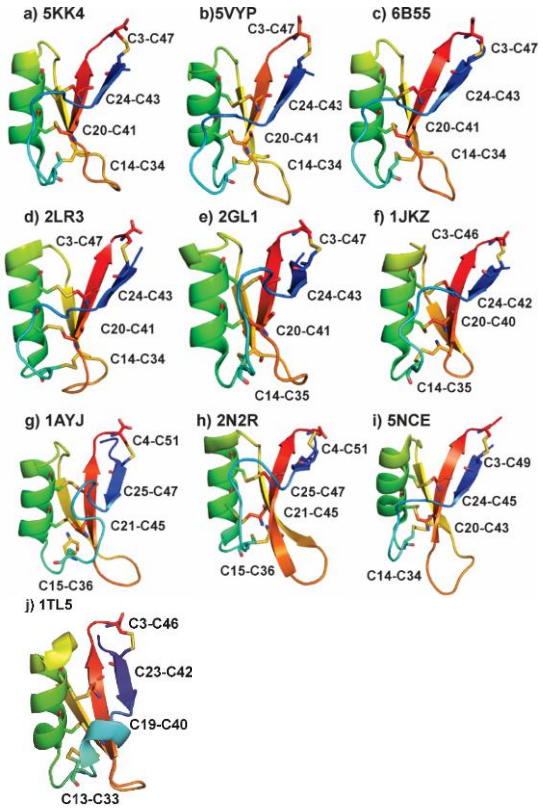

Source: Prepared by the author

action are still unclear, but the permeabilization of membrane bilayers containing negatively charged phospholipids occurs, as occurs similarly in the barrel-stave model (BROGDEN,

2005). Furthermore, recent studies suggest that the action of some defensins depends on their interaction with the membrane phospholipids, forming complexes such as NaD1-PIP2 (phosphatidylinositol 4,5-bisphosphate) (POON *et al*., 2014), MtDef4-PA (phosphatidic acid) (SAGARAM *et al*., 2013) and NsD7-PA (KVANSAKUL *et al*., 2016). These cases suggested that molecular structure of the defensins allow the recognition of phospholipids because an oligomeric cluster is formed after the recognition of the phospholipids by monomers. Therefore, the complex formation is capable of acting against the attack of microorganisms.

The mechanism of action of NaD1 on PIP2 cells involves the breakdown of membrane-cytoskeletal interactions mediated by the action of blebs (Payne *et al*., 2016). On the other hand, MtDef4 have a translocation signal in its sequence (RGFRRR amino acid sequence) that is needed for peptide internalization into cells (SAGARAM *et al*., 2013). Although these models aid to understand how the defensins mechanisms of action work, their relevance to how peptides damage and kill microorganisms still need to be elucidated.

Many studies are conducted out with plant defensins due to their diverse applications in different economic sectors (GHAG; SINGH SHEKHAWAT; GANAPATHI, 2015; MARMIROLI; MAESTRI, 2014; SHENKAREV *et al*., 2014; WANG *et al*., 2017). Since plant defensin are harmless for plants, these proteins may be used in different crops as a commercially viable approach for disease control in the agriculture (DE OLIVEIRA CARVALHO; MOREIRA GOMES, 2011). The works with defensins may provide molecular data that determine the effectiveness of defensins and thus making it possible to use in many fields as biotechnology, agriculture and medical applications. (KAUR; SAGARAM; SHAH, 2011). The use of mutagenesis technology to identify the molecular base of defensins is extremely time consuming (SOMAN; SIVAKUMAR; SREEKUMAR, 2010). However, the use of bioinformatics approach comes to help this experimental method, revealing the detailed energetic characterization of the defensins dimers involved in the complex with its ligant. This characterization is not available yet, thus this work would provide important information about the immunologic system of the plants.

The use of quantum methods coupled with classical methods in proteins have been shown to be relevant, showing that it is possible to reveal structural data and molecular mechanisms not exposed in the literature (ALAM *et al*., 2018; ZANATTA *et al*., 2014). Studies involving classical methods such as molecular dynamics provides information about the microscopic dynamic behavior which dependent on the time and individual atoms that constitute the system. Thus, it is possible to analyze the complexity of protein conformation ensemble in solution (BURKERT; ALLINGER, 1982; FOLKERS, 1994). When applied to

plant defensins, these methods could bring molecular and structural information which aid in biotechnology innovation (de Medeiros *et al*., 2010; Ermakova *et al*., 2016).

Furthermore, the quantum methods by themselves have been applied to biological systems mainly because high accuracy is required to estimate binding affinities. This type of method presents information at a level of complexity that is not capable of being revealed by purely classical methods (RAHA *et al*., 2007). Nevertheless, the numbers of atoms of large systems is still a challenge for QM method. To deal with this problem, DFT method is applied to describe the system by using its electron density ρ(r). Thus, the method does not use the full electronic wave function, instead the calculation depends on three spatial coordinates only (KOHN; SHAM, 1965; RAJAGOPAL; CALLAWAY, 1973). Besides, the Molecular Fractionation with Conjugated Caps (MFCC) scheme is a tool used in quantum calculations to reduce computational cost, because it fractionates the calculation that would be performed for large systems now for several micro systems (GORDON *et al*., 2012; HE; ZHANG, 2005a; ZHANG; ZHANG, 2003). In particular, our group has studied systems with the purpose of describing ligand−protein and protein-protein interactions at the quantum level in different biological systems (BARROSO-NETO *et al*., 2012; DANTAS *et al*., 2015; SOUSA *et al*., 2016; ZANATTA *et al*., 2014, 2016).

The crystal structure of the *Nicotiana suaveolens* defensin complexed with phosphatidic acid (PA) (NsD7-PA; pdb: 5KK4) reveals a striking double helix of two right-handed coiled oligomeric defensin fibrils (Figure 3). Kvansakul *et al* (2016) performed site-directed mutagenesis that targeted the: (i) type I PA-binding site, which the PA molecule is interaction in the junction between two neighboring NsD7 dimers; (ii) type II PA-binding site, which the PA is interacting in a cationic grip formed by each NsD7 dimer, (iii) isoleucine zipper, located on the inside of the oligomeric double helix and (iv) interoligomer region. Their findings revealed that the complex assembly is dependent upon the interaction with PA at the interface between NsD7 dimers. Also, they indicated that the defensin residues which define the stability of the NsD7: PA complex differ for the lipid engagement and for the dimer:dimer contacts (KVANSAKUL *et al*., 2016).

A recent study successfully applied the QM and MM method for the calculation of individual residue-residue interactions in biological systems (SOUSA *et al*., 2016). In this work, we established for the first time the composed residue-ligand-residue interaction by the quantum biochemistry method applied to defensin. In addition, we reveal for the first time the NsD7-PA comportment in silico by molecular dynamics method. Based on this approach, we were able to calculated the interaction between dimers of NsD7 complexed with PA.

6 MATERIALS AND METHODS

The input data for the calculations performed in this study was the X-ray crystal structure of plant defensin NsD7:PA complex (PDB ID: 5KK4) at 1.7 Å. The crystal structure is composed by three NsD7 dimers bound to six PA molecules in the asymmetric unit. The simulation was performed after the pairing of each helical coil via crystallographic symmetry with a second coil, forming a double- stranded defensin-lipid helix through PyMOL program. In this case, the complex NsD7-PA have in its structure six NsD7 dimers bounded by twelve PA molecules, as observed in figure 3.

The preparation of the molecular structure starts adding hydrogen atoms into NsD7:PA complex to fill any dangling bonds in the X-ray structure and their positions were optimized using classical molecular mechanics, with non-hydrogen species being kept frozen. After that, the determination of the protonation state of PA at physiological pH were accomplished using the Marvin Sketch code.

In order to calculate the interaction energy we selected parameters, including: (i) the semiempirical GGA+D exchange-correlation energy, which is able to take into account noncovalent forces such as hydrogen bonding and van der Waals interaction (DELLEY, 2000), (ii) The state of the art in semiempirical correction methods for dispersive forces is given by the Tkatchenko−Scheffler (TS) scheme, (TKATCHENKO *et al*., 2012) which accounts to some degree for the relative variation in dispersion parameters of differently bonded atoms, (iii) a double numerical plus polarization (DNP) basis set was adopted to expand the Kohn−Sham orbitals together with DFT semicore pseudopotentials, (iv) the orbital cutoff was set to 3.7 Å, and a total energy variation smaller than 10^{-6} Ha was assumed to achieve self-consistency, and (v) the geometry optimization, convergence tolerances were maximum energy variation smaller than 10^{-5} Ha, maximum force per atom smaller than 0.002 Ha/ Å, and maximum atomic displacement smaller than 0.005 Å.

The residue-residue−drug interaction energies were obtained by capping the isolated residues following the molecular fractionation with conjugate caps (MFCC) scheme which is a useful approach that provides an accurate description of biological systems through quantum calculations without a very high computational cost. (CHEN; ZHANG; ZHANG, 2005; GAO *et al*., 2004; HE; ZHANG, 2005b; ZHANG; ZHANG, 2003). Rodrigues and co-workers (2013) modified the method used to describe protein-protein interactions (RODRIGUES *et al*., 2013). This calculates the interaction energy between two specific residues (Ri and Rj) according to:

EI(Ri-Rj)=E(Ci-1RiCi+1Cj-1RjCj+1)-E(Ci-1RiCi+1Cj-1Cj+1) - E(Ci-1Ci+1Cj-1RjCj+1)+ E(Ci-1Ci+1Cj-1Cj+1) **(1)**

Figure 3 - NsD7-PA assembly represented in cartoon. The figure presents the oligomer composed by six dimers bound to twelve PA molecules, obtained from crystallographic data. The chains selected are represented by chain B (blue), chain A (green), chain C (magenta), chain H (forest), chain I (orange) and chain L (yellow). The phosphatidic acid molecule is represented in stick. The sticks colors are according to the chain to which it is situated.

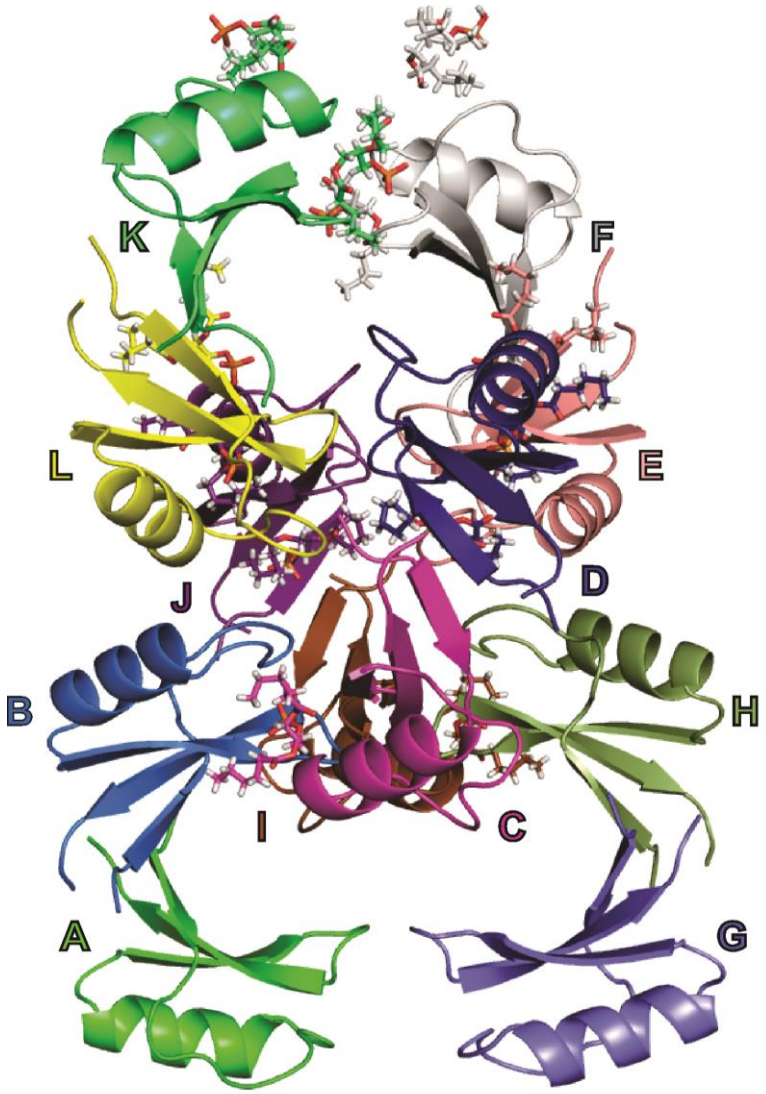

Source: Prepared by the author

In the above equation, the Ck terms refer to the conjugate caps, which must be chosen carefully to reproduce the local electronic environment of the amino acid residues (WU *et al*., 2007). In our study, these caps are the residues covalently bound to Rk;$C_{k \pm 1}$= $R_{k \pm 1}$ plus hydrogen atoms placed at any dangling bonds. At the right-hand side of eqn (1), the first term,

E (Ci-1 Ri Ci+1Cj-1 Rj Cj+1), is the total energy of the system formed by two interacting capped residues. The second term, E(Ci-1 Ri Ci+1 Cj-1 Cj+1), gives the total energy of the system formed by the capped residue Ri and the hydrogenated caps of Rj. The third term, E(Ci-1 Ci+1 Cj-1 Rj Cj+1), is the total energy of the system formed by Rj and the set of caps of Ri. Finally, E(Ci-1 Ci+1 Cj-1 Cj+1) is the total energy of the system formed by the caps only (RODRIGUES *et al*., 2013). Furthermore, in order to describe protein-protein-drug interactions, the PA molecule was added in the scheme, including its energy in the system. A new method was applied only when the PA molecule was at a distance of 3 angstrom between the residues to be calculated. Thus, the interaction energy between two specific residues (Ri and Rj) and the ligand (L) is according to eqn (2):

EI(Ri-Rj-L) = E(Ci-1 Ri Ci+1Cj-1 Rj Cj+1+L) -E(Ci-1 Ri Ci+1 Cj-1 Cj+1+L) - E(Ci-1 Ci+1 Cj-1 Rj Cj+1)+ E(Ci-1 Ci+1 Cj-1 Cj+1) **(2)**

Firstly in the equation 2, at the right-hand side of eqn (2), the first term, E(Ci-1 Ri Ci+1Cj-1 Rj Cj+1+L), is the total energy of the system formed by two interacting capped residues and ligand. The second term, E(Ci-1 Ri Ci+1 Cj-1 Cj+1+L), gives the total energy of the system formed by the capped residue Ri, the hydrogenated caps of Rj and ligand. As the equation 1, the third term, E(Ci-1 Ci+1 Cj-1 Rj Cj+1), is the total energy of the system formed by Rj and the set of caps of Ri. Lastely, E(Ci-1 Ci+1 Cj-1 Cj+1) is the total energy of the system formed by the caps only.

Following both schemes, the structural files obtained in protein data bank were prepared and used as input for calculations with DMOL3 code (DELLEY, 2000). The interaction energy between a specific pair of amino acid residues and the lingand was achieved from the total energies obtained for each system.

The chain chosen to be the target was the chain B (blue), which interacts with chain A (green), chain C (magenta), chain H (forest), chain I (orange) and chain L (yellow) (Figure 4 and 5). The chain B was chosen because of its position in the defensin assembly is shown to repeat in others points in the double-stranded defensin-lipid helix (Figure 3 and 4). A binding pocket radius R was defined, varying from 2.5 to 5.0 Å from the chain B, considering a distance-based binding interface. Thus, being supposed to contain the most important NsD7 residues witch interact in the interface between NsD7 chains with PA molecule (Figure 5). The selected distance range was reasoned on an average estimate that takes into account the fact that binding interactions in protein systems tend to become negligible at distances higher than 4.0 Å (ENGH; HUBER, 1991).

The Binding site, interaction energy, and residues domain (BIRD) pannel reveals some aspects of the residue-residue-ligand interaction follwing: (i) the interaction energy (in kcal/mol) for each selected amino acid residue is provided by the energy of all pairs of amino acids involved in their microsystems. The horizontal bars characterize the representation, from which one can visualize the relevance of each pair for the binding between strands, i.e.,

Figure 4 - Cartoon representation of chain B (blue), interacting with chain A (green), chain C (magenta), chain H (forest), chain I (orange) and chain L (yellow). The surface representation cover chain A, chain C, chain H, chain I and chain L, showing the selected chains which were used in calculations. The phosphatidic acid molecule (ACA101) is represented in stick colored magenta.

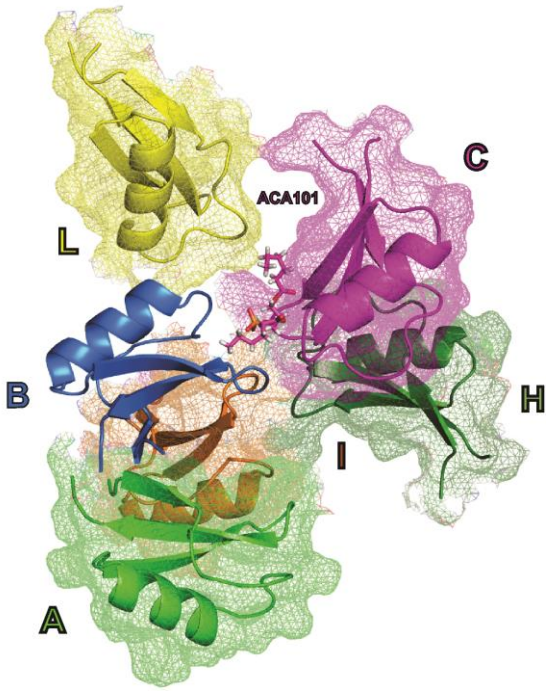

Source: Prepared by the author

their effectiveness, whether attracting or repelling each other; (ii) the labels of the amino acid residues, shown in the column at the left- hand side; and (iii) the amount of water molecules that were used to compose each microsystem to perform the interaction energy calculation, at the right-hand side column. In the calculation, the crystallographic water molecules were arranged within a range of 5.0 Å of the selected residues included. In addition, in each microsystem, the water molecule was positioned uniquely in the closest residue in the pair of interactions. Therefore, the interference of water molecules over the binding energy was estimated in the overall system. This method mimics the chemical environment for each amino acid with greater accuracy, providing a comparative basis for the contribution of water molecules over binding energies on the protein interface (SOUSA *et al*., 2016).

Therefore, the interference of water molecules over the binding energy was estimated in the overall system. This method mimics the chemical environment for each amino acid with greater accuracy, providing a comparative basis for the contribution of water molecules over binding energies on the protein interface (SOUSA *et al*., 2016). Here we performed all calculations using the COSMO continuum solvation model adopting a dielectric constant fixed. Recent study revealed that best fitted value of the dielectric constant for charge-charge interactions and for self-energies are in the range of $1< \varepsilon <40$. In our case, the simulations adopted ε value equals to 20.

Here we performed all calculations using the COSMO continuum solvation model adopting a dielectric constant fixed. Recent study revealed that best fitted value of the dielectric constant for charge-charge interactions and for self-energies are in the range of $1< \varepsilon$

Figure 5 - Representation in cartoon of Nsd7-PA complex. In this figure it is evident the interaction between chains. Chain B (blue) is interacting with chain A (green), chain C (magenta), chain H (forest), chain I (orange) and chain L (yellow). The representation in surface show the chain which the calculation was performed. The amino acid residues are represented in sticks. Some amino acid residues, which are in 5.0 Å of distance, are evidence in the figure. The sticks colors is according to the chain to which it is situated.

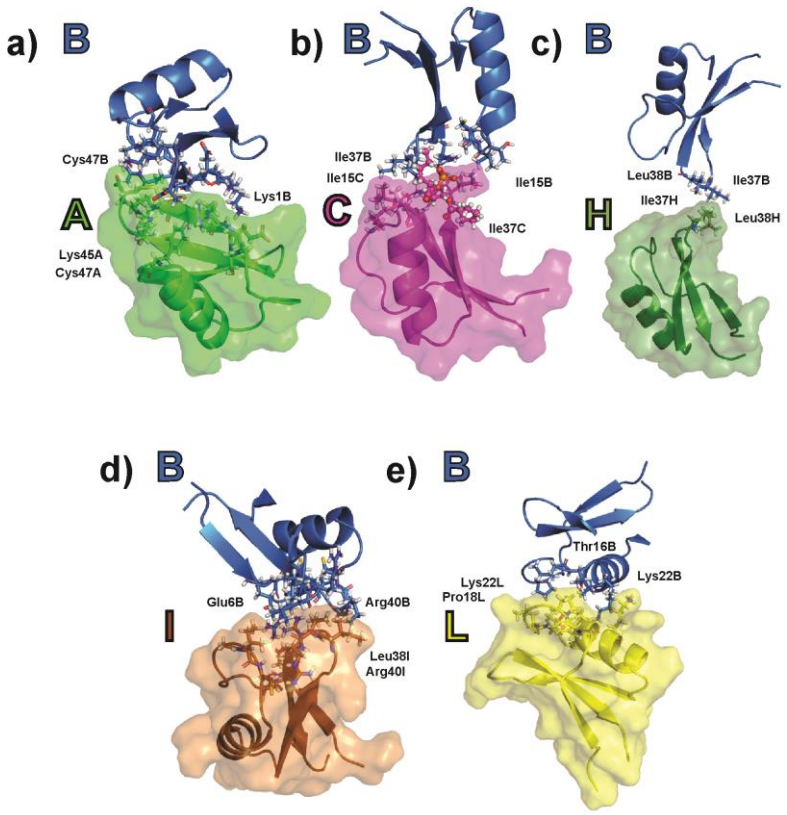

Source: Prepared by the author

<40. In our case, the simulations adopted ε value equals to 20. This method was applied to absolute folding free energies set of 45 proteins by Vicato *et al*, showing that is a practical and efficient technique (VICATOS; ROCA; WARSHEL, 2009).

In this study, we performed a molecular dynamic study to analyze the interaction and the stability of the NsD7 molecules in the presence or absence of the phosphatidic acid. The VMD program (Visual Molecular Dynamics) version 1.9.2 (HUMPHREY; DALKE; SCHULTEN, 1996) was used to prepare the files required in the simulation. Afterwards, VMD was used to analyze the simulation results. The simulations were configured according to the protocol used by Maranhão *et al* (2017) where, initially, the system was solved in a water box (model TIP3) with margins of 30 Å in each direction. After that, the load balancing and neutralization were made by the addition of sodium ions (Na +) and chloride (Cl^-). The amino acid residues of the NsD7 protein and PA molecules were flexible during dynamic. Two simulations were executed: (i) NsD7 in the absence PA. The dynamics were run at 300 K in 10.000 steps; (ii) NsD7 in the presence of PA. The dynamics was run at 300 K also in 10.000 steps. All the molecular dynamics simulations were executed under NTP (normal temperature and pressure) conditions.

The simulations were carried out using the NAMD program (Nanoscale Molecular Dynamics), version 2.9, using the CHARMM27 force field (MACKERELL *et al*., 1998; PHILLIPS *et al*., 2005). The evolution of the system was evaluated by RMSD (root mean square deviation), obtained through the VMD program (Visual Media Dynamics). The measurement of the RMSD expresses the variation in the position of the atoms of the system throughout the simulation time and, therefore, is considered an important parameter to evaluate the stability of the system (SALMAS; YURTSEVER; DURDAGI, 2015). RMSD measurements were taken considering the two systems mentioned above.

7 RESULTS AND DISCUSSION

Kvansakul *et al*. (2016) initialized the quantum biochemistry study of the defensin NsD7-PA complex using the X-ray crystal structure deposited in PDB (PDB: 5KK4). In order to characterize the structural basis of the NsD7:PA oligomer-fibril formation and understand the function in membrane permeabilization of NsD7-PA defensin, Kvansakul *et al*. (2016) performed experimental research using site-directed mutagenesis. Although, this previously work has helped to understand the NsD7-PA complex as a whole, the structural basis for triggering the oligomer, the role of specific ligands to induce the oligomer formation and the molecular structure of such defensin remains undefined (KVANSAKUL *et al*., 2016). This present work has motivated the residue-ligand-residue research through *in silico* simulations of NsD7-PA to reveal molecular information not available in literature yet.

DFT calculations were employed to analyze the relative energetic contribution of each pair of interactions, including PA energy, as well as the individual contribution of each amino acid residue, at chain B in relation to chain A (green), chain C (magenta), chain H (forest), chain I (orange) and chain L (yellow), from the NsD7-PA complex (Figure 4). The structural analysis of complex NsD7-PA detected 94 pair of interactions within a range of 5.0 Å including water residues (Table 1). The current strategy, using a distance-based binding interface, has found a few extra residues on NsD7-PA, beyond those previously mentioned in the literature (KVANSAKUL *et al*., 2016). The quantum analysis of the NsD7-PA complex revealed the binding energy of the following residues at chain B: K1, D2, C3, K4, R5, E6, S7, N8, F10, P11, G12, I13, C14, I15, T16, P18, P19, K22, F29, K36, I37, R39, L38, R40, C41, K45 and C47 (Figure 6).

Table 1 - Individual energetic contributions of all interactions involved in NsD7-PA complex including waters residues and chain where they are located.

B Residue	Interaction	Energy	Chain	B Residue	Interaction	Energy	Chain
K1	R5/w206	2.80	A	P18	K22	-1,2	L
K1	E6/w226	-16.00	A	P19	T16	-1.0	L
K1	S7/w223	-14.00	A	P19	P18	0.0	L
K1	N8/w209	-5.40	A	P19	P19	1.0	L
K1	R40/w237	3.0	A	K22/w501/w509	P18	-1.2	L
K1	L42	0.0	A	F29	C3	-5.0	A
D2	K4	1.0	A	F29	C47/w240/w201	-3.1	A
D2	R5/w206	-6.0	A	K36/w515	I15	-14.0	C
C3	C3	18.0	A	K36/w515	T16/w614	-6.1	C
C3	K4	0.0	A	K36/w515/ACA101	K36/w619	-4.1	C
C3	R5/w206	-4.0	A	K36/w515	I37/w605	0.3	C
C3	F29	-3.0	A	K36/w515/ACA101	R39	-2.2	C
C3	K45/w229	-3.2	A	I37	I13	-2.0	C

C3	C47	7.9	A	I37	T16/w614	0.0	C
K4	D2/w232/w202	-2.0	A	I37/ACA101	I15	1.0	C
K4	C3	1.0	A	I37/ACA101	K36/w619	-2.0	C
K4	K4	3.0	A	I37/ACA101	I37/w605	-2.0	C
K4	R5/w206	3.0	A	I37	R39	1.9	C
R5/w502/w514	K1/w214	-6.0	A	I37	I37	-1.0	H
R5/w502/w514	D2/w232/w202	-5.0	A	I37	L38	-1.5	H
R5/w502/w514	C3	-6.0	A	I37	I37	-1.0	I
R5/w502/w514	K4	2.0	A	L38	I37	-1.0	H
R5/w502/w514	P46	-1.0	A	L38	I13	3.0	I
R5/w502/w514	C47/w240/w201	-20.4	A	L38	I37	-2.0	I
E6/w518/w527	K1/w214	-7.0	A	L38	L38	-2.0	I
E6 w518/w527	L38	0.0	I	L38	R39	-11.0	I
E6 w518/w527	R40/w516/w716	-12.0	I	R39/w608/ACA101	K36/w619	-11.00	C
S7	R40/w516/w716	1.0	I	R39/w608	I37/w605	-2.00	C
N8/w518	K1/w214	3.8	A	R39/w608/ACA101	R39	-7.00	C
F10	L38	-0.5	I	R39	I37	0.0	I
F10	R40/w516/w716	-1.0	I	R39	L38	0.0	I
P11	T16/w835	-0.3	L	R39	R40/w516/w716	2.0	I
G12	L38	0.0	I	R40/w708	E6/w723	-3.0	I
G12	R40/w516/w716	-1.0	I	R40/w708	G12	0.0	I
I13/w530	I37/w605	-2.0	C	R40/w708	I13	-2.0	I
I13/w513/w530	I37	-2.0	I	R40/w708	C14	-8.0	I
I13/w513/w530	L38	-1.0	I	R40/w708	L38	0.0	I
C14	K36/w619	-6.0	C	R40/w708	R39	-8.0	I
C14	L38	-1.0	I	R40/w708	C41/w728	-1.0	I
I15/w517/ACA101	K36/w619	-4.0	C	C41/w523	L38	0.0	I
I15/w517	I37/w605	-1.0	C	C41/w523	R40/w516/w716	-7.0	I
I15/w517	I15/w825	-1.0	L	K45/w503/w511	C3	-15.0	A
T16/w529/ACA101	K36/w619	-1.0	C	K45/w503/w511	C47/w240/w201	14.4	A
T16	F10	-0.5	L	C47	K4	-5.2	A
T16	P11	-0.3	L	C47	R5/w206	-10.4	A
T16	P19	0.0	L	C47	F29	-7.3	A
P18	P19	0.0	L	C47	K45/w229	-17,9	A

Source: Prepared by the author

The BIRD panel (Figure 6) and the table below (Table 2) showed the sum of all interactions per residue selected at chain B in relation to the other residues in the neighborhood (top distance of 5.0 Å), revealing that interactions between residues are most attractive (negative charge). This result presents a relative high energy that enable assembly of the dimers into an oligomer.

Furthermore, it is possible to note that the most relevant interacting residues are Lys1 (-29.6 kcal mol-1), Arg5 (-36.4 kcal mol-1), Glu6 (-19.0 kcal mol-1), Lys36-PA (-26.1 kcal mol-1), Arg39-PA (-18.0 kcal mol-1), Arg40 (-24.0 kcal mol-1), Lys45 (-22.0 kcal mol-1), Cys47 (-26.0 kcal mol-1), which presents high attractive binding energy (Figure 6 and Table 2). Also, we reported throught Figure 7 all pairs of interaction between amino acid which reveled binding energy above 5.0 kcal mol-1.

Figure 6 - BIRD panel showing the MFCC interaction energy for all NsD7 amino acid residue. Light grey bars represent the binding energy values obtained ion the calculation. The distance of each interaction is presented at the right side of the panel. The number of water molecules involved for each interaction are presented at the right side of the panel.

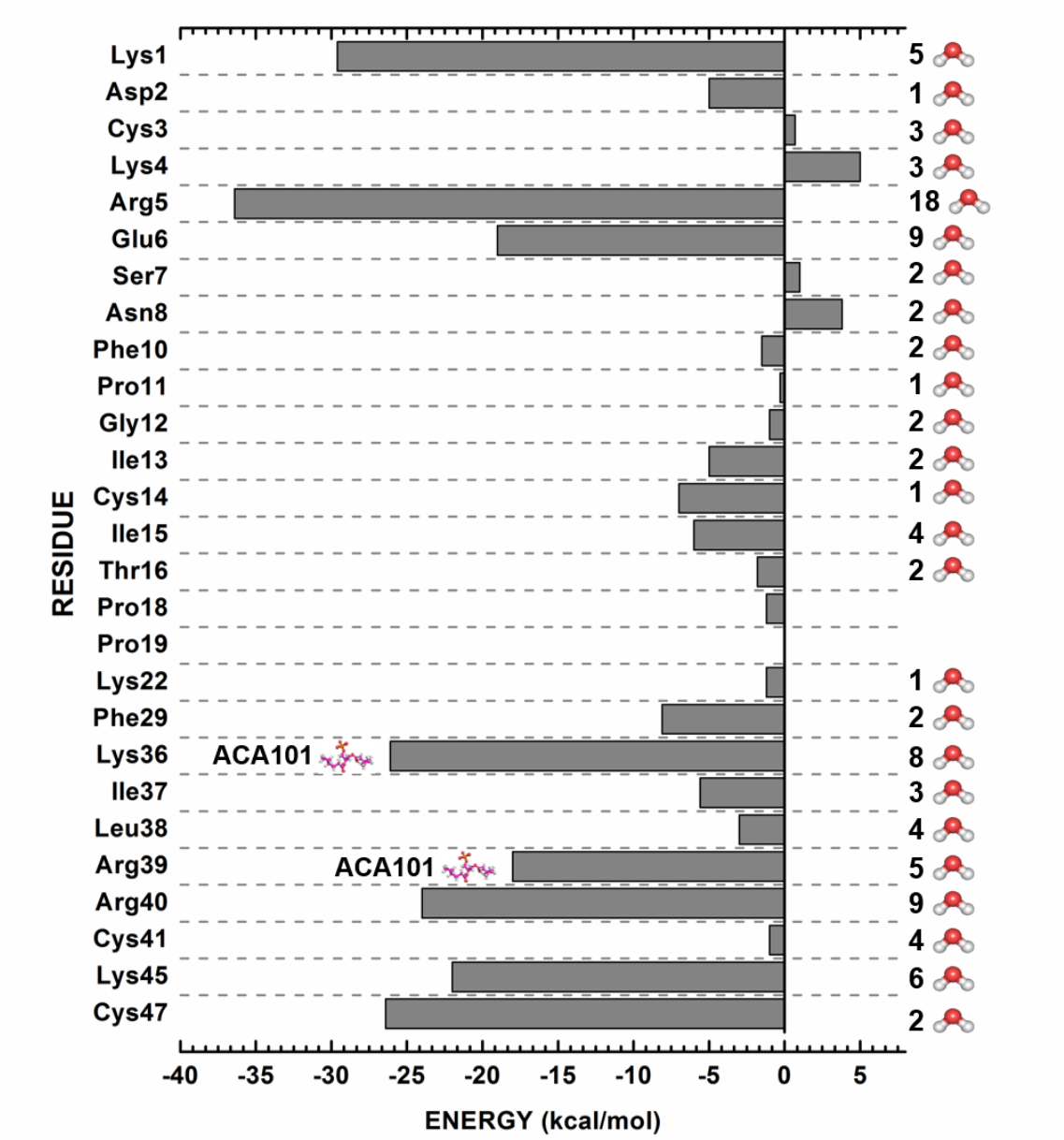

Source: Prepared by the author

Table 2 - Individual energetic contributions of Chain B amino acid residues involved in the interaction with residues selected in 5.0 Å of distance. Residues of chain A, chain C, chain H, chain I and chain L were selected.

Chain B residue	Interaction residue	Energy (kcal/ mol)	Interaction chain
K1	R5-A, E6-A, S7-A, N8-A, R40-A and L42-A.	-29.6	A
D2	K4-A and R5-A.	-5.0	A
C3	C3-A, K4-A, R5-A, F29-A, K45-A and C47-A.	0.7	A
K4	D2-A, C3-A, K4-A and R5-A.	5.0	A
R5/w502/w514	K1-A, D2-A, C3-A, K4-A, P46-A and C47-A	-36.4	A

E6/w518/w527	K1-A, L38-I and R40-I.	-19.0	A/I
S7	R40-I.	1.0	I
N8/w518	K1-A.	3.8	A
F10	L38-I and R40-I.	-1.5	I
P11	T16-L.	-0.3	L
G12	L38-I and R40-I.	-1.0	I
I13/w513/w530/ACA101-C	I37-C, I37-I and L38-I.	-5.0	C/I
C14	K36-C and L38-I.	-7.0	C/I
I15/w517	K36-C, I37-C and I15-L.	-6.0	C/L
T16/w529/w517/ACA101-C	K36-C, F10-L, P11-L and P19-L.	-1.8	C/L
P18	P19-L and K22-L.	-1.2	L
P19	T16-L, P18-L and P19-L.	0.0	L
K22/w501/w509	P18-L.	-1.2	L
F29	C3-A and C47-A.	-8.1	A
K36/w515/ACA101-C	I15-C, T16-C, K36-C, I37-C and R39-C.	-26.1	C
I37	I13-C, T16-C, K36-C, I37-C, R39-C, I37-H, L38-H and I37-I.	-5.6	C/H/I
L38	I37-H, I13-I, I37-I, L38-I and R39-I.	-3.0	H/I
R39/w608/ACA101-C	K36-C, I37-C, R39-C, I37- I, L38-I and R40-I.	-18.0	C/I
R40/W708	E6-I, G12-I, I13-I, C14-I, L38-I, R39-I and C41-I.	-24.0	H/I
C41/W523	L38-I and R40-I.	-1.0	I
K45/w503/w511	C3-A and C47-A.	-22.0	A
C47	C3-A, K4-A, R5-A, F29-A and K45-A.	-26.4	A

Source: Prepared by the author

Kvansakul *et al*. (2016) have reported that Lys36 and Arg39 residues, which are, located in type I PA-binding site, are the most important residues that allow assembly of the complex Nsd7-PA (KVANSAKUL *et al*., 2016). Our results corroborate with the previous study, seeing that both residues Lys36-PA (-26.1 kcal mol-1) and Arg39-PA (-18.0 kcal mol-1) revealed high attractive binding energy.

Furthermore, only Lys36 and Arg39 residues were under the new QM calculation method that involves directly PA molecule binding energy. For the very first time, the interaction protein-ligand-protein was described through QM methodology based on fragmentation. The calculation performed to the residue Lys36-PA, at chain B, was calculated with chain C residues (Ile15, Thr16, Lys36, Ile37 and Arg39) (Figure 8d). Differently, the calculation performed to the residue Arg39-PA, also at chain B, included chain C residues (Lys36, Ile 37 and Arg39) and chain I residues (Ile37, Leu38 and Arg 40) (Figure 9a). It is interesting to note that the interaction pairs between the chain C and the chain I showed nule or negative binding energy, revealing that the attraction between chain B and chain C are higher when compared with interaction between chain B and chain I at this binding site (Figure 9a).

Figure 7 - Binding site, interaction energy, and residues domain (BIRD) panel showing the MFCC interaction energy for all interactions established above 5.0 kcal mol^{-1} between dimers of NsD7-PA complex. Dark bars represent values obtained with ε = 20. The number of water molecules involved for each interaction are presented at the right side of the panel.

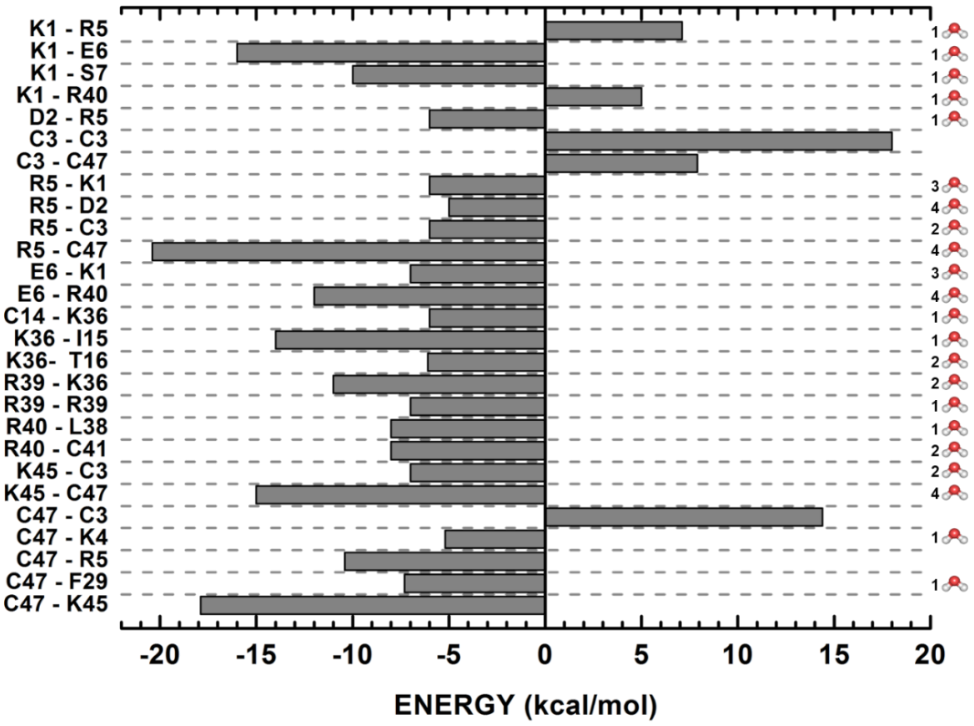

Source: Prepared by the author

In the previous literature, the residues Lys1 (-29.6 kcal mol^{-1}), Arg5 (-36.4 kcal mol^{-1}), Glu6 (-19.0 kcal mol^{-1}), Arg40 (-24.0 kcal mol^{-1}), Lys45 (-22.0 kcal mol^{-1}) and Cys47 (-26.0 kcal mol^{-1}) do not present a remarkable influence over the complex formation (Figure 4 and Table 2). However, these residues have strong attractive interactions, indicating that these residues are relevant for the complex formation. Besides, these findings suggest that site-directed mutagenesis in this residues can cause the loss of fibril formation of the complex Nsd7-PA. On the other hand, Kvansakul *et al*. (2016) showed the relevance of Ile15 and Ile37 residues, located at the isoleucine zipper, for fibril formation, as well as our study demonstrated that these both residues, with individual contributions of -6.0 kcal mol^{-1} and -5.8 kcal mol^{-1}, respectively, are relevant for the stability of the complex at this binding site (Figure 4 and Table 2). In addition, the QM analysis on Lys4 showed that it does not appear to interfere directly with the NsD7 association. The binding energy calculated for this residue was 5.0 kcal mol^{-1}, displaying a low repulsive interaction (Figure 4 and Table 2). These findings

revalidate the previous study, which showed that the site-directed mutagenesis on the Lys4 residue (located at type II PA-binding site) did not show ablation of oligomer formation.

Figure 8 - Main amino acid residues involved in the monomers interaction. The interaction energy are represented in the BIRD panels. At the left side present the MFCC interaction energy for each residue interaction performed by Lys1 (a), Arg5 (b), Glu6 (c) and Lys36 (d), all located in chain B. The residues, which interact with the residues of the B chain, are represented close to the chain where they are located, also at the left side of the panel. Light grey bars represent values obtained in the quantum calculation. The residue coordinations are represented at the right side as sticks, showing their interaction with residue belonging to the chain B residue (represented as ball and sticks colored blue).

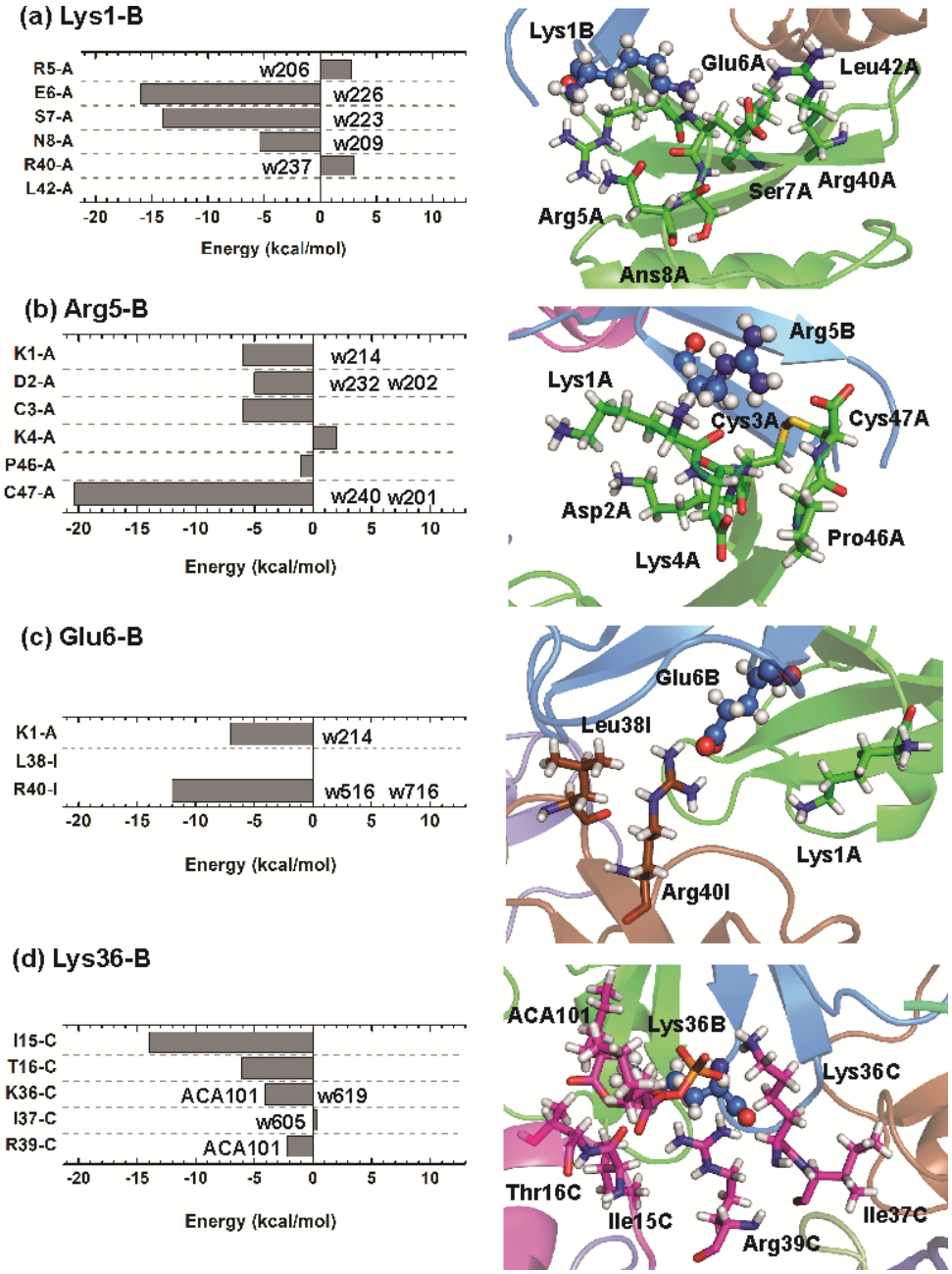

Source: Prepared by the author

Figure 9: Main amino acid residues involved in the monomers interaction. The interactions energy are represented in the BIRD panel. At the left side present the MFCC interaction energy for each residue interaction performed by Arg39 (a), Arg40 (b), Lys45 (c) and Cys47 (d), all located in chain B. The residues, which interact with the residues of the B chain, are represented close to the chain where they are located, also at the left side of the panel. Light grey bars represent values obtained in the quantum calculation. The residue coordinations are represented at the right side as sticks, showing their interaction with residue belonging to the chain B residue (represented as ball and sticks colored blue).

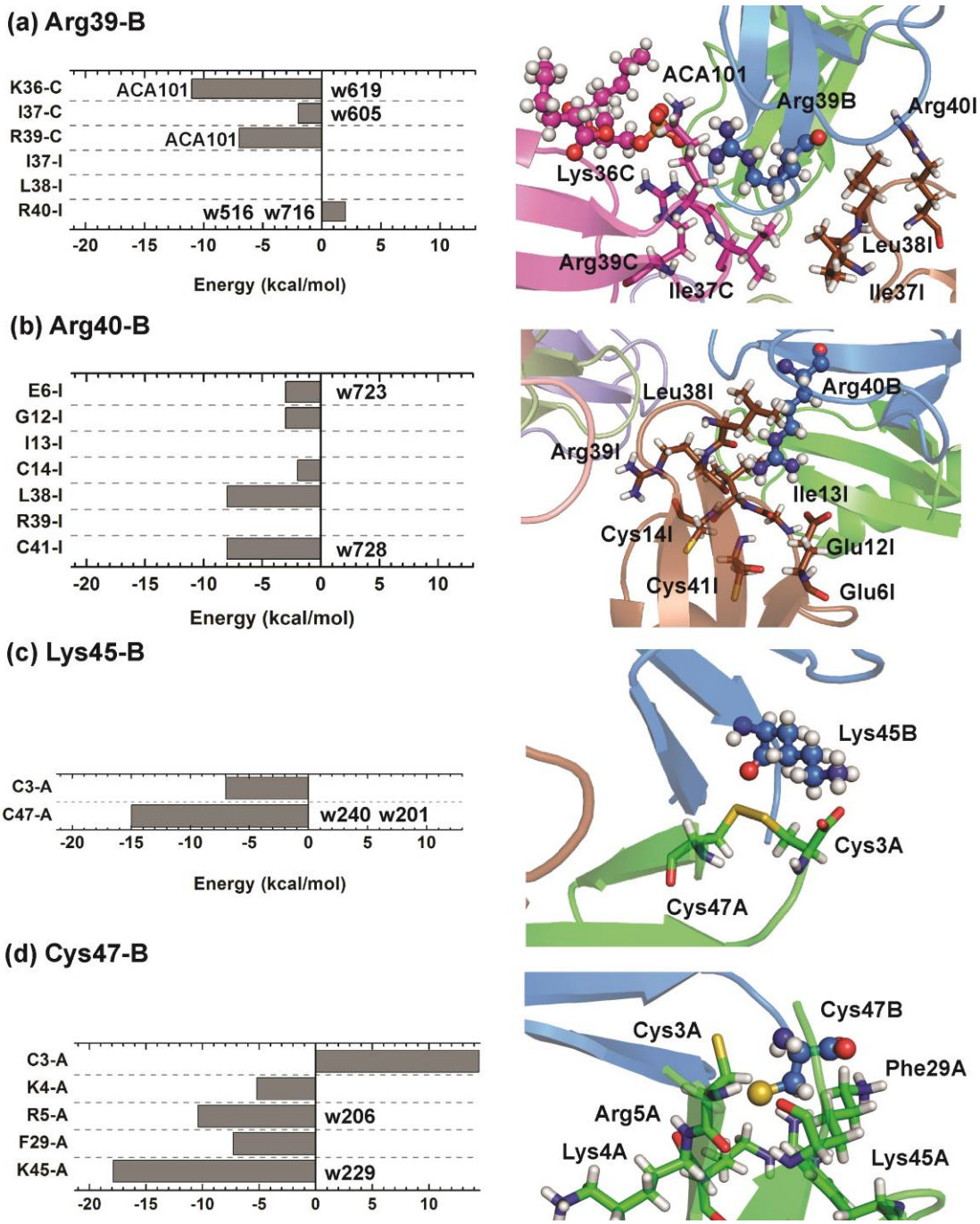

Source: Prepared by the author

In order to check the hypothesis of dimers dissociation in the absence of PA molecule, we performed, for the first time, a classical molecular dynamics simulation applied to NsD7-PA system. Simulations were performed in 10 ns each, and the distance among dimers and some residues were used to monitor the stability of the orientation. We noticed that NsD7-PA complex in the presence of PA molecule showed considerable stability during 10ns of simulation. On the other hand, we observed lower stability in NsD7 in the absence of PA molecule, also performed in 10ns of simulation. In the NsD7 analysis, the instability caused changes in the geometry, which induced dimers separation (Figure 10). Thus, the high level of dimers detachment observed in NsD7, when compared with NsD7-PA, reveals the low stability in the system that PA is not present. We noticed the dimers stability in the system through RMSD values in figure 10. While RMSD results showed 2.3 Å variation for NsD7, in the NsD7-PA complex it was observed only 1.97 Å variation. These results exposed that the NsD7 system showed greater variation with respect to the point of origin than NsD7-PA system. It is possible to compare the systems behavior between the beginning and the end of dynamics simulations for the both systems in Figure 10.

Figure 10 - RMSD of Nsd7 in the absence of PA molecule (a) and Nsd7 in the presence of PA molecule (b) during 10 ns of molecular dynamics.

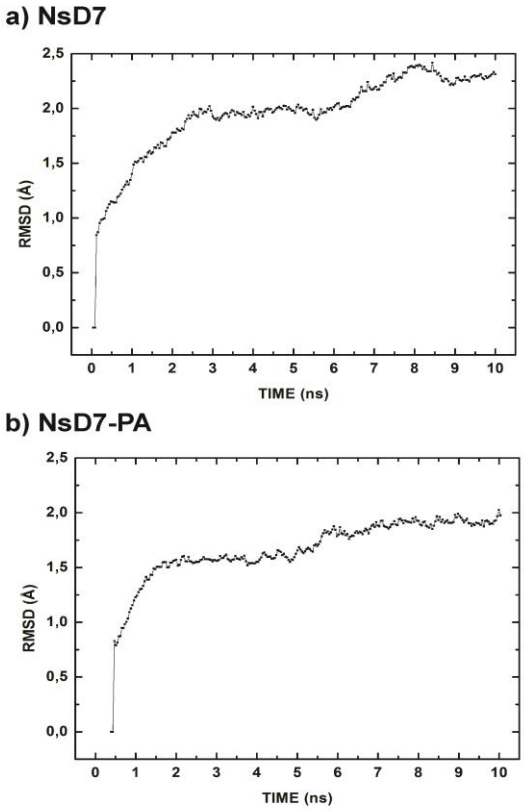

Source: Prepared by the author

As observed in Figure 11**,** the complex NsD7-PA underwent a small conformational change due to only permittivity of the free space and relative dielectric constant of the medium. In a different way, it occurred in the NsD7 system where there was a greater system ablation as previously mentioned (Figure 11). In this manner, it suggests that the absence of PA molecule in the defensin complex impact on defensin functionality.

Figure 11: Cartoon representation of MD simulation. The starting position of both dynamics (frame 2) are colored in magenta. (a) Cartoon representation of NsD7in the absence of Pa molecule. The final position are colored green. (b)Cartoon representation of NsD7 complex with Pa molecule. The final position are colored blue. The ball and stick are representing PA molecules. It is colored according to the dynamics position to which it is situated.

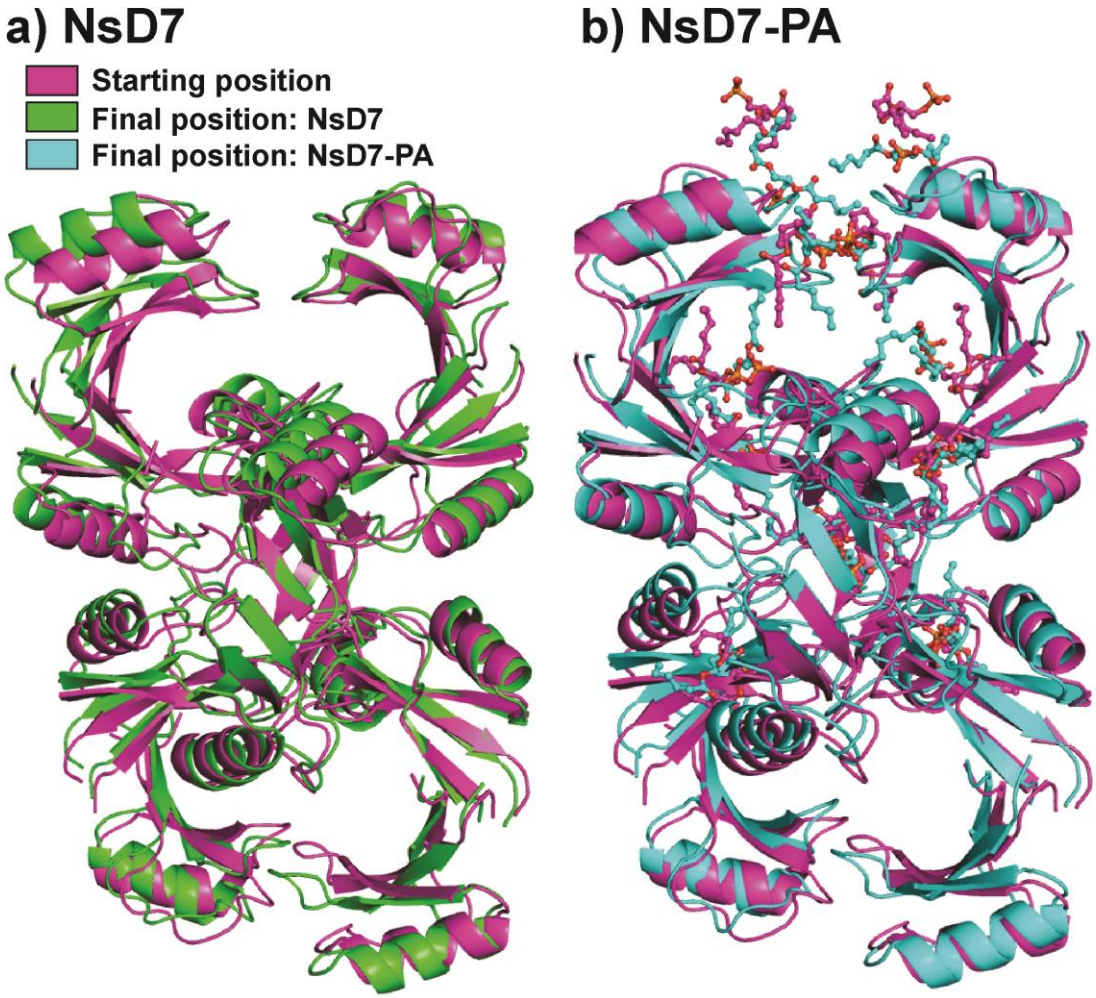

Source: Prepared by the author

Molecular Dynamics results also revealed some important differences when amino acid residues were analyzed in 10ns of simulation. Figure 12 shows in a global way the movement of amino acid residues, which compose different chains at the end of both simulation in NsD7 and NsD7-PA. In such manner, it was possible to evaluate the system as a whole analyzing specific residues. In this manner, we compared the residues ablation between simulations performed in NsD7 and NsD7-PA: the interaction between Arg21 (chain J) and Ala23 (chain B) showed separation of 3.3 Å; the interaction between Arg21 (chain C) and Ala23 (chain K) showed separation of 6.2 Å; and the interaction between Lys36 (chain K) and Arg40 (chain L) showed separation of 2.5 Å. The local differences observed in the distances between residues reveal changes in the overall system (Figure 12).

Figure 12 - Cartoon transparence represent the final position of NsD7 MD simulation (colored green). Cartoon transparence represents the final position of NsD7-PA MD simulation (colored blue). The ball and stick are representing amino acid residues. It is colored according to the NsD7 complex to which it is situated. Residue−Residues distances are depicted by black dashed lines.

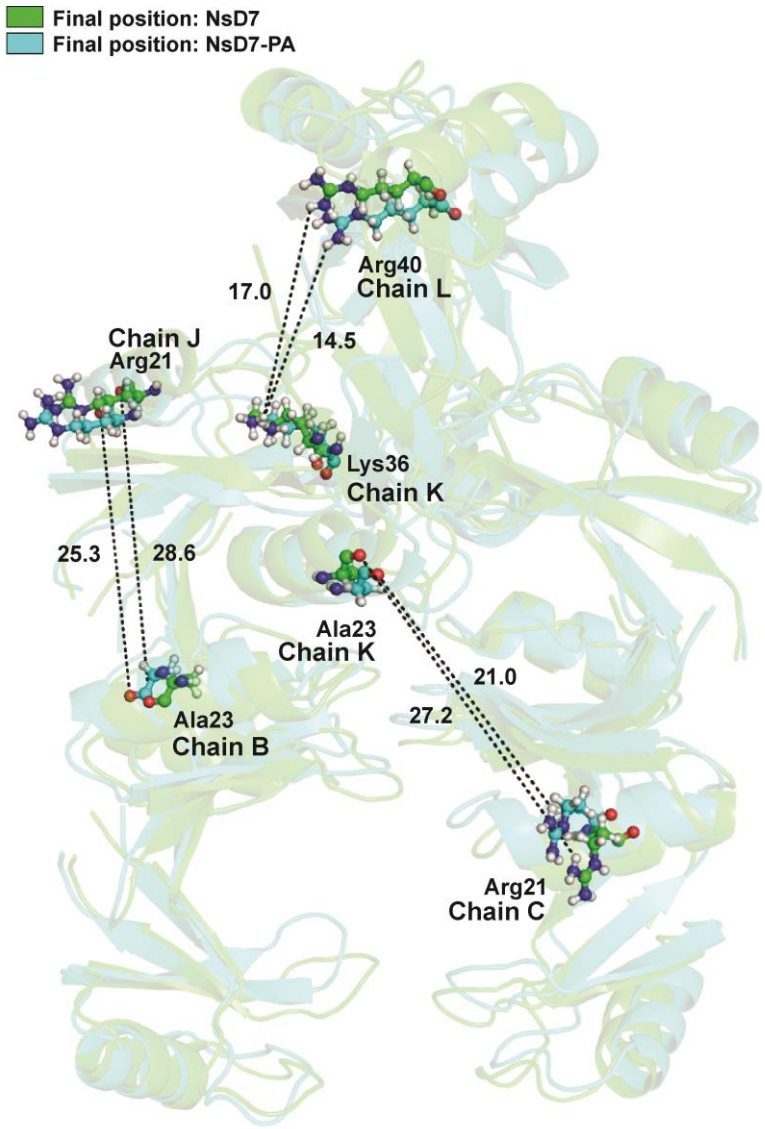

Source: Prepared by the author

This work also was capable to merge Quantum Mechanics study with Molecular Dynamics study through amino acid residues analysis. The Figure 13 revealed some changes in the distance between amino acid residues which that had their energies calculated by quantum mechanics. As mentioned previously, the QM study revealed the binding energy of pair residues Lys36 (chain B) - Arg39 (chain C) and Arg5 (chain B) - Cys47 (chain A), with values of -2.2 kcal.mol^{-1} and -20.0 kcal.mol^{-1}, respectively (Figure 8). Before MD simulation (blue cartoon), the pairs Lys36 (chain B) - Arg39 (chain C) were at 11.6 Å of distance and Arg5 (chain B) - Cys47 (chain A) were at 7.6 Å of distance. We noticed that after MD simulation (green drawing) the distances between all residues were more distant in relation to the beginning of the MD (Figure 13). In the case of Lys36 (chain B) - Arg39 (chain C) we noticed 0.9 Å distance variation. This value is higher than the value established for Arg5 (chain B) - Cys47 (chain A) pair, that revealed only 0.2 Å distance variation. The distance variation between these pairs of residues corroborate with QM result, which showed higher binding energy for Arg5 (chain B) - Cys47 (chain A) pair (-20 kcal.mol^{-1}) than compared with binding energy of Lys36 (chain B) - Arg39 (chain C) pair (-2.2 kcal.mol^{-1}) (Figure 8 and Figure 13).

Figure 13 - Cartoon transparence represents the final position of NsD7 MD simulation (colored green). Cartoon transparence represents the final position of NsD7-PA MD simulation (colored blue). The ball and stick are representing amino acid residues. It is colored according to the NsD7 complex to which it is situated. Residue−Residues distances are depicted by black dashed lines.

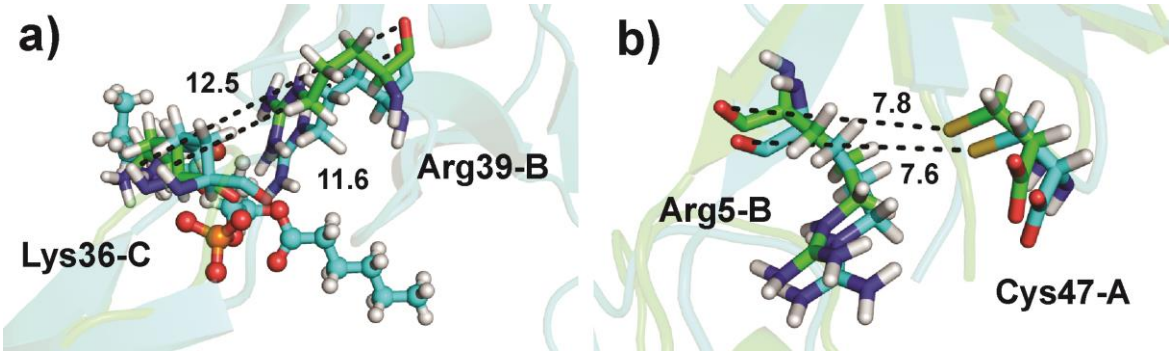

Source: Prepared by the author

8 CONCLUSION

The current analysis outlines a detailed energetic description of NsD7-PA complex, deepening our knowledge about the defensin immune system, NsD7. Moreover, our results have provided a structural and energetic basis of NsD7 defensin. In this manner, it is possible extend the same approach to others defensins in order to expand the knowledge about immune system of plants with the intention of improving. Quantum calculations have confirmed the importance of PA molecule in the oligomerization mainly through the residues that interact with PA molecule in the system. It was observed through the Lys36 and Arg39 residues, which showed high energy of interaction. These assumptions corroborate Kvansakul *et al*. (2016) study, which performed experimental research using site-directed mutagenesis to prove that Lys36 and Arg39 residues are important in the oligomer-fibril formation (KVANSAKUL *et al*., 2016).

Furthermore, others residues, never mentioned in literature, had its importance revealed in QM analysis, such as: Lys1 (-29.6 kcal mol-1), Arg5 (-36.4 kcal mol-1), Glu6 (-19.0 kcal mol-1), Arg40 (-24.0 kcal mol-1), Lys45 (-22.0 kcal mol-1) and Cys47 (-26.0 kcal mol-1). These residues showed attractive binding energy, which suggest their dimers. All this facts emphasizes the crucial role of these residues jointly with PA molecule in the importance in the assembly and stabilization of NsD7-PA complex. After performing quantum mechanics, we also performed classical molecular dynamics, showing that in the absence of PA molecule had disruptions of residues interactions, causing dimers detachments. When compared with simulation of NsD7-PA complex, the NsD7 by itself had more abrupt changes in its secondary structure conformation. It leaded to system instability proved by RMSD graphic, which may cause a severe impact on defensin functionality. Overall, our results demonstrate, for the first time, that the new QM method applied to NsD7 system is practical to elucidate molecular data never shown in previous literature. Moreover, the computational techniques at the quantum level jointly with classical molecular dynamics methods can be very useful to provide molecular data that determine the effectiveness of defensins and thus making it possible to use in many fields as biotechnology, agriculture and medical applications. In the future, both approaches should search alternatives molecules that binding and promoting the oligomerization in others defensins systems expanding defensins knowledge and thus improving the immune system of plants.

REFERENCIES

ALAM, M. *et al*. DFT/TD-DFT calculations, spectroscopic characterizations (FTIR, NMR, UV-vis), molecular docking and enzyme inhibition study of 7-benzoyloxycoumarin. **Computational Biology and Chemistry**, Seoul v. 73, p. 65-78, 2018.

BARROSO-NETO, I. L. *et al*. Inactivation of ovine cyclooxygenase-1 by bromoaspirin and aspirin: A quantum chemistry description. **Journal of Physical Chemistry B**, Fortaleza, v. 116, n. 10, p. 3270-3279, 2012.

BLOCH, C.; RICHARDSON, M. A new family of small (5 kDa) protein inhibitors of insect alpha-amylases from seeds or sorghum (Sorghum bicolar (L) Moench) have sequence homologies with wheat gamma-purothionins. **FEBS letters**, Durham, v. 279, n. 1, p. 101-104, 1991.

BOMAN, H. G.; HULTMARK, D. Cell-free immunity in insects. **Trends in Biochemical Sciences**, New York, v. 6, p. 306-309, 1981.

BROGDEN, K. A. Antimicrobial peptides: Pore formers or metabolic inhibitors in bacteria**.** **Nature Reviews Microbiology**, Iowa City, v. 3, p. 238-250, 2005.

BURKERT, U.; ALLINGER, N. L. Molecular Mechanics. **Accurate Molecular Structures Their Determination and Importance**, Chester, v. 117, p. 1-10, 1982.

CHEN, G. H. *et al*. Cloning and characterization of a plant defensin VaD1 from azuki bean. **Journal of Agricultural and Food Chemistry**, Taiwan, v. 53, n. 4, p. 982-988, 2005.

CHEN, X.; ZHANG, Y.; ZHANG, J. Z. H. An efficient approach for ab initio energy calculation of biopolymers. **Journal of Chemical Physics**, New York, v. 122, n. 18, 2005.

DANTAS, D. S. *et al*. Quantum molecular modelling of ibuprofen bound to human serum albumin. **RSC Advances**, Natal, v. 5, n. 61, p. 49439-49450, 2015.

DE MEDEIROS, L. N. *et al*. Backbone dynamics of the antifungal Psd1 pea defensin and its correlation with membrane interaction by NMR spectroscopy. **Biochimica et Biophysica Acta - Biomembranes**, Rio de Janeiro, v. 1798, n. 2, p. 105-113, 2010.

DE OLIVEIRA CARVALHO, A.; MOREIRA GOMES, V. Plant Defensins and Defensin-Like Peptides - Biological Activities and Biotechnological Applications. **Current Pharmaceutical Design**, New York, v. 17, n. 38, p. 4270-4293, 2011.

DELLEY, B. From molecules to solids with the DMol3 approach. **The Journal of Chemical Physics**, Villigen, v. 113, n. 18, p. 7756-7764, 2000.

ENGH, R. A.; HUBER, R. Accurate bond and angle parameters for X-ray protein structure refinement. **Acta Crystallographica Section A**, *[s.l]*, v. 47, n. 4, p. 392-400, 1991.

ERMAKOVA, E. A. *et al*. Structure of Scots pine defensin 1 by spectroscopic methods and computational modeling. **International Journal of Biological Macromolecules**, Kazan, v. 84, p. 142-152, 2016.

FOLKERS, G. Molecular modeling. In: FOLKERS, G. **Molecular modeling:** Basic principles and applications. Edição 3. Düsseldorf: Editora Wiley-VCH, 2008. v. 49

GAO, A. M. *et al*. An efficient linear scaling method for ab initio calculation of electron density of proteins. **Chemical Physics Letters**, New York, v. 394, n. 4-6, p. 293-297, 2004.

GHAG, S. B.; SINGH SHEKHAWAT, U. K.; GANAPATHI, T. R. Plant Defensins for the Development of Fungal Pathogen Resistance in Transgenic Crops. In: GHAG, S. B. **Genetically Modified Organisms in Food**. Mumbai: Editora AP books, 2015. p.381-396

GORDON, M. S. *et al*. Fragmentation methods: A route to accurate calculations on large systems. **Chemical Reviews**, Ibaraki, v. 112, n.1, p. 632–672, 2012.

HE, X.; ZHANG, J. Z. H. A new method for direct calculation of total energy of protein. **The Journal of chemical physics**, Nanjing, v. 122, n. 3, p. 31103, 2005.

HÖGLUND, P.; LJUNGGREN, H. G. Natural killer cells in cancer. In: **Natural Killer Cells**. *[s.l: s.n.*]. p. 55-64.

HUMPHREY, W.; DALKE, A.; SCHULTEN, K. VMD: Visual molecular dynamics. **Journal of Molecular Graphics**, Urbana, v. 14, n. 1, p. 33-38, 1996.

KAUR, J.; SAGARAM, U. S.; SHAH, D. Can plant defensins be used to engineer durable commercially useful fungal resistance in crop plants? **Fungal Biology Reviews**, Saint Louis, v. 25, n. 3, p. 128-135, 2011.

KOHN, W.; SHAM, L. J. Self-consistent equations including exchange and correlation effects. **Physical Review**, San Diego, v. 140, n. 4A, 1965.

KUSHMERICK, C. *et al*. Functional and structural features of gamma-zeathionins, a new class of sodium channel blockers. **Febs Letters**, Belo Horizonte, v. 440, n. 3, p. 302-306, 1998.

KVANSAKUL, M. *et al*. Binding of phosphatidic acid by NsD7 mediates formation of helical defensin-lipid oligomeric assemblies and membrane permeabilization. **Proceedings of the National Academy of Sciences of the United States of America**, Melbourne, v. 113, n. 40, p. 11202-11207, 2016.

MACKERELL, A. D. *et al*. All-Atom Empirical Potential for Molecular Modeling and Dynamics Studies of Proteins. **The Journal of Physical Chemistry B**, Cambridge, v. 102, n. 18, p. 3586-3616, 1998.

MARMIROLI, N.; MAESTRI, E. Plant peptides in defense and signaling. **Peptides**, Parma, v. 56, p. 30-44, 2014.

MIROUZE, M. *et al*. A putative novel role for plant defensins: A defensin from the zinc hyper-accumulating plant, Arabidopsis halleri, confers zinc tolerance. **Plant Journal**, Auzeville-Tolosane, v. 47, n. 3, p. 329-342, 2006.

PHILLIPS, J. C. *et al*. Scalable molecular dynamics with NAMD**. Journal of Computational Chemistry**, Urbana, v. 26, n. 16, p. 1781-1802, 2005.

POON, I. K. H. *et al*. Phosphoinositide-mediated oligomerization of a defensin induces cell lysis. **eLife**, Melboune, v. 2014, n. 3, 2014.

RAHA, K. *et al*. The role of quantum mechanics in structure-based drug design. **Drug Discovery Today**, Gainesville, v. 12, n. 17-18, p. 725-731, 2007.

RAJAGOPAL, A. K.; CALLAWAY, J. Inhomogeneous electron gas. **Physical Review B**, Baton Rouge, v. 7, n. 5, p. 1912-1919, 1973.

RODRIGUES, C. R. F. *et al*. Quantum biochemistry study of the T3-785 tropocollagen triple-helical structure. **Chemical Physics Letters**, Fortaleza, v. 559, p. 88-93, 2013.

SAGARAM, U. S. *et al*. Structural and functional studies of a phosphatidic acid-binding antifungal plant defensin MtDef4: Identification of an RGFRRR motif governing fungal cell entry. **PLoS ONE**, Saint Louis v. 8, n. 12, 2013.

SALMAS, R. E.; YURTSEVER, M.; DURDAGI, S. Investigation of inhibition mechanism of chemokine receptor CCR5 by micro-second molecular dynamics simulations. **Scientific Reports**, Istanbul, v. 5, n. 13180, p. 1-12, 2015.

SEGURA, A. *et al*. Novel defensin subfamily from spinach (Spinacia oleracea). **FEBS Letters**, Madrid, v. 435, n. 2-3, p. 159-162, 1998.

SHENKAREV, Z. O. *et al*. Heterologous expression and solution structure of defensin from lentil Lens culinaris. **Biochemical and Biophysical Research Communications**, Moscow, v. 451, n. 2, 2014.

SOMAN, S. S.; SIVAKUMAR, K. C.; SREEKUMAR, E. Molecular dynamics simulation studies and in vitro site directed mutagenesis of avian beta-defensin Apl_AvBD2. **BMC bioinformatics**, v. 11, n. 1, 2010.

SOUSA, B. L. *et al*. Explaining RANKL inhibition by OPG through quantum biochemistry computations and insights into peptide-design for the treatment of osteoporosis. **Rsc Advances**, Fortaleza, v. 6, n. 88, p. 84926-84942, 2016.

SPELBRINK, R. G. Differential Antifungal and Calcium Channel-Blocking Activity among Structurally Related Plant Defensins. **Plant physiology**, St. Louis, v. 135, n. 4, p. 2055-2067, 2004.

THOMMA, B. P. H. J.; CAMMUE, B. P. A.; THEVISSEN, K. Plant defensins. **Planta**, Heverlee-Leuven, v. 216, n. 2, p. 193-202, 2002.

TKATCHENKO, A. *et al*. Accurate and Efficient Method for Many-Body van der Waals Interactions. **Physical Review Letters**, Berlin, v. 108, n. 23, p. 236402-236407, 2012.

VICATOS, S.; ROCA, M.; WARSHEL, A. Effective approach for calculations of absolute stability of proteins using focused dielectric constants. **Proteins**, Los Angeles, v. 77, n. 3, p.

670-84, 2009.

WANG, G. Improved methods for classification, prediction, and design of antimicrobial peptides. **Computational Peptidology**. *[s.l: s.n.*]. p. 43-66.

WANG, Q. *et al*. Overexpression of Jatropha curcas Defensin (JcDef) Enhances Sheath Blight Disease Resistance in Tobacco. **Journal of Phytopathology**, Chengdu, v. 165, n. 1, p. 15-21, 2017.

WIJAYA, R. *et al*. Defense proteins from seed of Cassia fistula include a lipid transfer protein homologue and a protease inhibitory plant defensin. **Plant Science**, Bundoora, v. 159, n. 2, p. 243-255, 2000.

WU, E. *et al*. Quantum and Molecular Dynamics Study for Binding of Macrocyclic Inhibitors to Human α-Thrombin. **Biophysical Journal**, Dalian, v. 92, p. 4244-4253, 2007.

ZANATTA, G. *et al*. Antipsychotic haloperidol binding to the human dopamine D3 receptor: Beyond docking through QM/MM refinement toward the design of improved schizophrenia medicines. **ACS Chemical Neuroscience**, Porto Alegre, v. 5, n. 10, p. 1041-1054, 2014.

ZANATTA, G. *et al*. Two Binding Geometries for Risperidone in Dopamine D3 Receptors: Insights on the Fast-Off Mechanism through Docking, Quantum Biochemistry, and Molecular Dynamics Simulations. **ACS Chemical Neuroscience**, Porto Alegre, v. 7, n. 10, p. 1331-1347, 2016.

ZHANG, D. W.; ZHANG, J. Z. H. Molecular fractionation with conjugate caps for full quantum mechanical calculation of protein-molecule interaction energy. **Journal of Chemical Physics**, Singapore, v. 119, n. 7, p. 3599-3605, 2003.

ZHANG, Y.; LEWIS, K. Fabatins: New antimicrobial plant peptides. **FEMS Microbiology Letters**, Cambridge, v. 149, n. 1, p. 59-64, 1997.